Therapeutic efficacy of FASN inhibition in preclinical models of HCC

Haichuan Wang, Yi Zhou, Hongwei Xu, Xue Wang, Yi Zhang, Runze Shang, Marie O'Farrell, Stephanie Roessler, Carsten Sticht, Andreas Stahl, Matthias Evert, Diego F. Calvisi, Yong Zeng, Xin Chen

Supporting Materials

Table of Contents

Supplementary Materials and Methods……..…..……2

Supplementary Tables S1-6……..……..…….……11

Supplementary Figure Legends……..……..…18

Supplementray Figures S1-38……..……..……..…29

Supplementary Materials and Methods

Constructs and reagents

The plasmids used in this study, including px330-Cas9-sgPTEN, pT3-EF1α-c-MET (human c-MET), pT3-EF1α-ΔN90-β-Catenin (with N terminal Myc-tag), pT3EF1α-c-MYC, pT3-EF1α-HA-myr-AKT (with N terminal HA-tag), pT2CAGGS-NRASV12, and pCMV-Sleeping beauty transposase (SB), have been described previously in detail [1]. Cabozantinib (Cat# C-8901, LC Laboratories, Woburn, Massachusetts, USA) was dissolved in 30% PEG400/H_2O (PEG400, Poly[ethylene glycol], Cat#202398, Millipore Sigma, Burlington, Massachusetts, USA; diluted in ddH2O at 3:7 v/v ratio) to generate a working solution of 12 mg/mL. Sorafenib (Cat# S8502, LC Laboratories, Woburn, Massachusetts, USA) was prepared as an 8 mg/mL working solution. Detailed information on the sorafenib formulation used in this study can be accessed via https://pharm.ucsf.edu/xinchen/protocols/sorafenib-formulation. Anti-mouse PD-L1 antibody was obtained from Genentech (South San Francisco, California, USA), while control IgG was purchased from BioXcell (West Lebanon, NH). The antibodies were diluted in cold PBS at a 1:9 v/v ratio with a final concentration of 10 mg/ml before use. TVB-3664 (3-V Biosciences, Menlo Park, California, USA) was dissolved in 100% PEG400 to a 6 mg/ml stock solution. The TVB3664 stock solution can be stocked at room temperature for 7 days, and it was diluted in ddH_2O at a 3:7 v/v ratio every day before dosing. C75 (Cat# C5490) was purchased from Sigma-Aldrich, St. Louis, MO, USA. Cabozantinib, TVB3664, and C75 were dissolved in DMSO for *in vitro* experiments.

Hydrodynamic injection and mouse treatment

The wild-type *FVB/N* mice were obtained from Charles River Laboratories (Wilmington, MA). The *Fasn*$^{flox/flox}$ conditional knockout mice in C57BL/6J genetic background were described previously

[2]. Sleeping beauty (SB)-mediated hydrodynamic tail vein injection was conducted as previously described [1]. Briefly, plasmid-normal saline (0.9%NaCl) mixed solution was injected into 5.5- to 8-week-old mice in 5~7 seconds, with the total volume equal to 0.1ml/g body weight.

To determine the effects of TVB3664 on aged livers, ~40 weeks old *FVB/N* wild-type mice were used. The mice were treated with TVB3664 (N=5; 10mg/kg/day) or vehicle (N=5) through oral gavage. One treatment cycle includes 6 consecutive dosing days and 1 day of washout. Mice were sacrificed after 3 cycles of treatment. The serum and liver samples were collected for biochemical and histological analysis.

To establish the AKT model (Fig. 1), both male and female *Fasn*$^{flox/flox}$ mice were applied. The amounts of plasmids for injection were: 10μg pT3-EF1a-HA-AKT plasmids (mouse) and 40μg pCMV-Cre (or 40μg pCMV empty vector) and 2μg pCMV-SB. Mice were treated with TVB3664 (10mg/kg/day) or vehicle at 1-week post-injection (w.p.i) through oral gavage. One treatment cycle includes 6 consecutive dosing days and 1 day of washout. Mice were sacrificed at 1 w.p.i (no treatment), 2 w.p.i (1 cycle), 3 w.p.i (2 cycles), 4 w.p.i (3 cycles) and 5 w.p.i (3 cycles and 1-week rest), respectively. For each group at each time point, a total of 3~5 mice were harvested for analysis.

For the HCC therapeutic studies, 5.5- to 8-week-old mice female *FVB/N* mice were used. For the murine HCC models, the amounts of plasmid for injection are: (sgPTEN/c-MET model) 40μg pX330-Cas-sgPTEN and 20μg pT3-EF1α-c-MET plasmids (human) along with 0.8μg pCMV-SB, (AKT/NRAS model) 15μg pT3-EF1α-HA-myr-AKT plasmids and 15μg pT2CAGGS-NRasV12 plasmids (human) along with 1.2μg pCMV-SB, (c-MYC model) 10μg pT3EF1α-c-MYC plasmids mixed with 0.4μg pCMV-SB, (β-CateninΔ90/ c-MET) 20μg pT3-EF1α-c-MET plasmids (human) and 20μg pT3-EF1α-ΔN90-β-Catenin plasmids along with 1.6μg pCMV-SB. TVB3664 (10mg/kg/day), cabozantinib (60mg/kg/day), cabozantinib (60mg/kg/day) + TVB3664 (10mg/kg/day), sorafenib (30mg/kg/day), sorafenib (30mg/kg/day)+ TVB3664 (10mg/kg/day) or

vehicle was orally administered via gavage. Anti-mouse PD-L1 Ab (or isotype IgG) was injected from tail vein with 20mg/kg for the first dose and intraperitoneally injected twice a week with 10mg/kg for the following five doses. Therapy starting points were determined based on pilot experiments and our previous studies [3, 4]. One treatment cycle includes 6 consecutive dosing days and 1 day of washout. Mice were sacrificed after 3 cycles of treatment. Mice were housed, fed, and monitored according to protocols approved by the Committee for Animal Research at the University of California San Francisco (San Francisco, CA, USA), protocol number AN185770. The abdominal girth and the signs of morbidity or discomfort were monitored for all mice.

Cell culture and *in vitro* studies

HLE, MHCC97H, and SNU449 human HCC cell lines were used for the *in vitro* studies. The HLE cell line was purchased from the JCRB Cell Bank, whereas SNU449 cell lines were purchased from ATCC. The MHCC97H cell line was a kind gift from Dr. Binbin Liu from Fudan University, Shanghai, China. Cell lines were validated (Genetica DNA Laboratories, Burlington, NC, USA) and tested clear of mycoplasma contamination. Cells were cultured in Dulbecco's modified Eagle medium (DMEM; Gibco, Grand Island, NY, USA) with 10% fetal bovine serum (FBS; Gibco, Grand Island, NY, USA), 100 U/mL penicillin, and 100 g/mL streptomycin (Gibco) at 37 °C in a 5% CO_2 humidified incubator. For IC50 determination, cells were seeded in 24-well plates and treated with a gradient concentration of cabozantinib, TVB3664, or C75 in triplicate for 48 hours. Then cells were enumerated by crystal violet staining. After washing, stained cells were incubated in lysis solution and shaken gently on a rocking shaker for 20–30 min. Diluted lysate solutions were added to 96-well plates, and the OD was measured at 590 nm with the BioTek ELX808 Absorbance Microplate Reader (ThermoFisher Scientific, Waltham, MA, USA). Determination of the combination index was performed as previously described [5]. In brief, HCC cells were treated with a series concentration of cabozantinib and/or TVB3664 or C75. The overall inhibitory effects were

used to calculate the combination index (CI). CI < 1 indicates a synergistic effect by the combination treatment. For Western blot analysis, cells were treated with DMSO, cabozantinib, TVB3664, or cabozantinib/TVB3664 for 48 hours and then harvested for analysis.

Fatty acid uptake assay

Oleic acid (Cat# O-7501, Sigma-Aldrich, St. Louis, MO) was used for *in vitro* fatty acid uptake assay. The bovine serum albumin (BSA)-conjugated oleic acid solution was prepared using a modified method based on Listenberger *et al.* (PMID: 11278654). In brief, oleic acid was dissolved in 0.01M NaOH solution and incubated at 70° for 30 minutes for making a 60mM stocking solution. The working solutions were freshly prepared before each fatty acid challenge. First, the oleic acid stocking solution was complexed with 5% (wt/vol) fatty acid-free BSA (Cat# A6003, Sigma, St. Louis, MO) in phosphate-buffered saline (PBS) (1:9, v/v) to achieve a final concentration of 6mM. Next, the complexed oleic acid was added to the serum-containing cell culture medium (1:5, v/v) to accomplish an oleic acid concentration of 1mM. The control solution was prepared by complexing 0.01 M NaOH solution with 5% (wt/vol) fatty acid-free BSA in PBS (1:9, v/v). According to Listenberger *et al.*, the pH of the medium did not differ significantly with the addition of complexed fatty acid. For the fatty acid uptake assay, the HLE, MHCC97H, and SNU449 human HCC cell lines were seeded in 24-well culture plates and challenged with oleic acid for 24 hours. After the oleic acid challenge, cells were fixed and subjected to Oil-Red-O staining.

RNA extraction and quantitative real-time polymerase chain reaction (qPCR)

Total mRNA from mouse liver tissues was extracted with the Quick RNA miniprep kit (Zymo Research, Irvine, CA, USA), following the manufactures' instructions. Next, mRNA expression was detected by quantitative real-time polymerase chain reaction (qPCR) using SYBR Green

Master Mix (Applied Biosystems, Foster City, CA, USA) in a QuantStudio™ 6 Flex system (Applied Biosystems). The expression of each gene was normalized with the 18S rRNA. Thermal cycling started with an initial hold period at 95°C for 10 minutes and then followed by a three-step PCR program of 95°C for 15 seconds, 60°C for 1 minute, and 72°C for 30 seconds for a total of 40 cycles. The primers used are listed in Supporting Table S4.

RNASeq analysis

RNA samples used for RNA sequencing were isolated from murine sgPTEN/c-MET HCCs treated with vehicle (VEH; N=4), cabozantinib (CAB; N=4), TVB3664 (TVB; N=4), cabozantinib/TVB3664 (COM; N=4) as well as *FVB/N* wild-type normal livers (FVB; N=3). RNA was extracted using the Zymo Quick-RNA Miniprep Kit (Cat# D7001, Zymo Research, Irvine, CA), followed by quantification with Nanodrop. The RNA quality control was determined using Agilent RNA 6000 Nano Kit (Agilent Technologies, Santa Clara, CA, USA) and the Bioanalyzer (Agilent Technologies, Santa Clara, CA UAS). Library preparation and sequencing were performed by Novogene (Sacramento, CA, USA). Poor quality reads were trimmed using the fastq-mcf (1.05) [6, 7]. Reads quality was checked using the fastqc (v0.11.7). We aligned reads to the respective genome (mm10) using STAR (version 2.6.0). Gene read counts were in Ensemble ID and converted to Entrez ID using the Bioconductor Package Maintainer org.Mm.eg.db, version 3.8.2. Duplicated and not annotated genes were removed. Data were filtered out with genes with row means less than 5. The edgeR package was used for the fpkm calculation, data normalization, and differentially expressed genes identification [8, 9]. The differential expression was limited by a p-value of 0.05 and LogFC of $Log_2(1.5)$. The Venn diagram was initially drawn using the VennDiagram package [10] and then reconstructed by Venn Diagram Plotter (https://omics.pnl.gov/software/venn-diagram-plotter). Heatmaps and Kyoto Encyclopedia of Genes and Genomes (KEGG) analysis were drawn using the gplots package [11]. Furthermore,

pathway analysis of canonical pathways and upstream regulators was performed with Ingenuity Pathway Analysis (Qiagen, Hilden, Germany).

Protein extraction and Western blot analysis

For total protein extraction, the detailed procedures can be accessed via https://pharm.ucsf.edu/xinchen/protocols/protein-extraction. In brief, mouse liver tissues and cells were homogenized in M-PER™ Mammalian Protein Extraction Reagent (Cat# 78501, Thermo Fisher Scientific, Waltham, MA, USA) containing the Halt™ Protease Inhibitor Cocktail (Cat# 78429, Thermo Fisher Scientific, Waltham, MA, USA). The protein concentrations were determined with the Pierce™ Microplate BCA Protein Assay Kit (Cat#23252, Thermo Fisher Scientific, Waltham, MA, USA), following the manufacturer's instructions. For Western blotting, extracted proteins were boiled in Laemmli sample buffer (2X; Cat# 1610737, Bio-Rad Laboratories, Hercules, CA, USA) for denaturation, separated by SDS-PAGE (Cat# M00654, GenScript, Piscataway, NJ, USA), and transferred onto nitrocellulose membranes using the Trans-Blot Turbo Transfer System and RTA Transfer Packs (Cat# 1704271, Bio-Rad Laboratories, Hercules, CA, USA). Membranes were blocked with 10% non-fat dry milk in Tris-buffered saline containing 0.05% Tween-20 for 1-2 hours at room temperature and then incubated with primary antibodies (summarized in Supporting Table S5) at 4°C overnight. Membranes were then incubated with horseradish peroxidase-secondary antibody (1:5000; Jackson ImmunoResearch Laboratories Inc., West Grove, PA) at room temperature for 1 hour. After appropriate washing, membranes were developed with the ClarityTM Western ECL Substrate (Cat#170-5061, Bio-Rad Laboratories, Hercules, CA, USA) or ClarityTM Max Western ECL Substrate (Cat#170-5062, Bio-Rad Laboratories, Hercules, CA, USA). Western blots were quantified using the ImageJ software (Version 1.51n, National Institutes of Health, Bethesda, MD, https://imagej.nih.gov/ij), as previously described [12].

Histology, immunohistochemistry, and Oil-Red-O staining

A board-certified pathologist and liver expert (M.E.) conducted the histopathologic examination of the mouse lesions, following the criteria by Frith *et al.* [13]. Antigen unmasking was achieved by placing the slides in a microwave oven on high for 10 min, either in 10 mM sodium citrate buffer (pH 6.0) or 1mM ethylenediaminetetraacetic acid (EDTA; pH 8.5), followed by a 20 min cool down at room temperature. After a blocking step with 5% goat serum and Avidin-Biotin blocking kit (Vector Laboratories, Burlingame, CA), the slides were incubated with primary antibodies overnight at 4°C. Slides were then subjected to 3% hydrogen peroxide for 10 min to quench endogenous peroxidase activity. Subsequently, the biotin-conjugated secondary antibody was applied at a 1:500 dilution for 30 min at room temperature. The antibodies used are described in Supporting Table S6. Immunoreactivity was visualized with the Vectastain Elite ABC kit (Cat#PK-6100, Vector Laboratories) and ImmPACT® DAB Peroxidase (HRP) Substrate (Cat#SK-4105, Vector Laboratories). Slides were counterstained with hematoxylin. Proliferation and apoptosis indices were determined in mouse HCC lesions by counting Ki-67 and Cleaved Caspase 3 positive cells, respectively. ImageJ 1.8.0 (National Institutes of Health, USA, https://imagej.nih.gov/ij/download.html) and the Image Pro Plus 7 (Media Cybernetics, Rockville, MD) software were used for quantification, respectively. For Oil-Red-O staining, detailed information can be accessed via https://pharm.ucsf.edu/xinchen/protocols/oil-red-o. In brief, Liver tissues were embedded in optimum cutting temperature compound (Tissue-Tek, Sakura Finetek, Torrance, CA) and frozen in cold 2-Methylbutane at -80°C. Frozen sections were cut at 5μm in thickness. Oil Red O (Item# KTORO, American MasterTech Scientific Laboratory Supplies, Lodi, CA) staining was performed on frozen sections according to the standard instructions.

Serum biochemical assays and assessment of hepatic cholesterol, triglycerides,

The serum liver panel, including alanine aminotransferase (ALT), aspartate aminotransferase (AST), alkaline phosphatase (ALKP), total protein (TP), and albumin (ALB) levels and serum lipid panels, including cholesterol (CHOL), triglyceride (TRIG), low-density lipoprotein (LDL) and high-density lipoprotein cholesterol (HDLC) were performed using standard clinical protocol by the Clinical Laboratory at Zuckerberg San Francisco General Hospital (San Francisco, CA). In addition, the hepatic cholesterol and triglyceride levels in sgPTEN/c-MET and c-MYC models were assessed using the Cholesterol Quantitation Kit and the Triglyceride Quantification Kit (BioVision Inc., Mountain View, CA, USA), respectively, following the manufacturer's recommendation.

Human HCC TCGA data retrieval and analysis

To investigate *PTEN* expression levels, liver hepatocellular carcinoma (TCGA, PanCancer Atlas) data at the public cBioPortal site (https://www.cbioportal.org/) were utilized. Samples with *PTEN* mRNA expression data (354 patients/samples) were obtained. With the adoption of median value, TCGA HCC samples were categorized into $PTEN^{High}$ (N=197) and $PTEN^{Low}$ (N=197) expression groups. The analysis of MET activation status was performed as previously described [14]. In brief, human samples with expression data, including surrounding non-tumor liver tissues (ST) from both TCGA-LIHC and TCGA-CHOL database and primary HCCs from the TCGA-LICH database [15], were retrieved from the TGCG data set. A gene set containing 18 genes upregulated in liver cancer samples upon c-MET activation was developed. The expressions of these genes were standardized and ordered by ascending Average of 18-gene expression of each sample from left to right. The weight of each gene was defined as 1 in this gene set. Samples with Averages greater than the Average + 1.5 SD of the ST were considered as MET^{High} HCC. Updated follow-

up survival data were downloaded using the R package TCGAbiolinks. Kaplan-Meier survival data were evaluated using a log-rank (Mantel-Cox) test. The Prism 7.0 software (GraphPad, San Diego, CA) was used for data analysis.

References

1. Chen X, Calvisi DF. Hydrodynamic transfection for generation of novel mouse models for liver cancer research. Am J Patho 2014;184:912-923.
2. Chakravarthy MV, Zhu Y, López M, Yin L, Wozniak DF, Coleman T, et al. Brain fatty acid synthase activates pparα to maintain energy homeostasis. J Clin Invest 2007;117:2539-2552.
3. **Shang R, Song X, Wang P**, Zhou Y, Lu X, Wang J, et al. Cabozantinib-based combination therapy for the treatment of hepatocellular carcinoma. Gut 2021;70:1746.
4. Calvisi DF, Wang C, Ho C, Ladu S, Lee SA, Mattu S, et al. Increased lipogenesis, induced by AKT-mTORC1-RPS6 signaling, promotes development of human hepatocellular carcinoma. Gastroenterology 2011;140:1071-1083.e1075.
5. Song X, Liu X, Wang H, Wang J, Qiao Y, Cigliano A, et al. Combined CDK4/6 and pan-mTOR inhibition is synergistic against intrahepatic cholangiocarcinoma. Clinical Cancer Research 2019;25:403.
6. Aronesty E. Titile. 2011. https://github.com/ExpressionAnalysis/ea-utils
7. Aronesty E. Comparison of sequencing utility programs. Open Bioinforma J 2013;7:1-8.
8. Robinson MD, McCarthy DJ, Smyth GK. Edger: A bioconductor package for differential expression analysis of digital gene expression data. Bioinformatics 2010;26:139-140.
9. McCarthy DJ, Chen Y, Smyth GK. Differential expression analysis of multifactor RNA-seq experiments with respect to biological variation. Nucleic Acids Research 2012;40:4288-4297.
10. Chen H. Titile. 2018. https://CRAN.R-project.org/package=VennDiagram
11. Galili T, Jongbloets A, Pilosov M. Titile. 2021. https://github.com/talgalili/gplots
12. **Wang H, Wang J,** Zhang S, Jia J, Liu X, Zhang J, et al. Distinct and overlapping roles of Hippo effectors YAP and TAZ during human and mouse hepatocarcinogenesis. Cellular and Molecular Gastroenterology and Hepatology 2021;11:1095-1117.
13. Frith CH, Ward JM, Turusov VS. Tumours of the liver. IARC Sci Publ 1994:223-269.
14. Qiao Y, Wang J, Karagoz E, Liang B, Song X, Shang R, et al. Axis inhibition protein 1 (Axin1) deletion–induced hepatocarcinogenesis requires intact β-Catenin but not NOTCH cascade in mice. Hepatology 2019;70:2003-2017.
15. Ally A, Balasundaram M, Carlsen R, Chuah E, Clarke A, Dhalla N, et al. Comprehensive and integrative genomic characterization of hepatocellular carcinoma. Cell 2017;169:1327-1341.e1323.

Author names in bold designate shared co-first authorship.

Supporting Table S1. KEGG analysis of down regulated genes in TVB3664 treated- compared to those in the vehicle treated- sgPTEN/c-MET tumors.

Entry	Pathway Name	N	DE	P.DE	Enrichment
path:mmu01100	Metabolic pathways	1574	20	0.003041	1.27064803
path:mmu00830	Retinol metabolism	97	4	0.00428	4.12371134
path:mmu04915	Estrogen signaling pathway	134	4	0.013158	2.985074627
path:mmu00980	Metabolism of xenobiotics by cytochrome P450	73	3	0.013506	4.109589041
path:mmu00230	Purine metabolism	136	4	0.013831	2.941176471
path:mmu04918	Thyroid hormone synthesis	74	3	0.014009	4.054054054
path:mmu03060	Protein export	29	2	0.01661	6.896551724
path:mmu04710	Circadian rhythm	30	2	0.017719	6.666666667
path:mmu04612	Antigen processing and presentation	90	3	0.023514	3.333333333
path:mmu00983	Drug metabolism - other enzymes	92	3	0.024896	3.260869565
path:mmu00350	Tyrosine metabolism	40	2	0.030418	5
path:mmu04659	Th17 cell differentiation	105	3	0.034929	2.857142857
path:mmu00620	Pyruvate metabolism	44	2	0.036257	4.545454545
path:mmu00071	Fatty acid degradation	52	2	0.049092	3.846153846

Abbreviations: KEGG,Kyoto Encyclopedia of Genes and Genomes; N, number of pathway genes in total; DE, number of differentially expressed genes; P.DE, p value of defferentially expressed genes.

Supporting Table S2. KEGG analysis of down regulated genes in cabozantinib treated- compared to those in the vehicle treated- sgPTEN/c-MET tumors.

Entry	Pathway Name	N	DE	P.DE	Enrichment
path:mmu04015	Rap1 signaling pathway	214	16	5.04E-06	7.476635514
path:mmu04218	Cellular senescence	184	14	1.65E-05	7.608695652
path:mmu05200	Pathways in cancer	543	26	2.38E-05	4.788213628
path:mmu04010	MAPK signaling pathway	294	17	7.24E-05	5.782312925
path:mmu04141	Protein processing in endoplasmic reticulum	172	12	0.000155	6.976744186
path:mmu04014	Ras signaling pathway	232	13	0.000705	5.603448276
path:mmu05220	Chronic myeloid leukemia	76	7	0.000746	9.210526316
path:mmu05215	Prostate cancer	99	8	0.000759	8.080808081
path:mmu05143	African trypanosomiasis	39	5	0.000972	12.82051282
path:mmu04934	Cushing syndrome	162	10	0.001417	6.172839506
path:mmu04612	Antigen processing and presentation	90	7	0.00202	7.777777778
path:mmu05169	Epstein-Barr virus infection	231	12	0.002147	5.194805195
path:mmu05222	Small cell lung cancer	93	7	0.002438	7.52688172
path:mmu05224	Breast cancer	147	9	0.002579	6.12244898

Abbreviations: KEGG,Kyoto Encyclopedia of Genes and Genomes; N, number of pathway genes in total; DE, number of differentially expressed genes; P.DE, p value of defferentially expressed genes.

Supporting Table S3. KEGG analysis of down regulated genes in cabozantinib/TVB3664 combinational treated- compared to those in the vehicle treated- sgPTEN/c-MET tumors.

Entry	Pathway Name	N	DE	P.DE	Enrichment
path:mmu04110	Cell cycle	125	16	0.000391	12.8
path:mmu04750	Inflammatory mediator regulation of TRP channels	127	16	0.000468	12.5984252
path:mmu05222	Small cell lung cancer	93	13	0.00058	13.97849462
path:mmu05200	Pathways in cancer	543	44	0.000654	8.103130755
path:mmu00830	Retinol metabolism	97	13	0.000872	13.40206186
path:mmu04014	Ras signaling pathway	232	23	0.001025	9.913793103
path:mmu04926	Relaxin signaling pathway	129	15	0.001602	11.62790698
path:mmu04068	FoxO signaling pathway	131	15	0.00187	11.45038168
path:mmu03060	Protein export	29	6	0.00246	20.68965517
path:mmu05223	Non-small cell lung cancer	72	10	0.002571	13.88888889
path:mmu04115	p53 signaling pathway	72	10	0.002571	13.88888889
path:mmu05204	Chemical carcinogenesis - DNA adducts	84	11	0.002577	13.0952381
path:mmu04151	PI3K-Akt signaling pathway	359	30	0.002984	8.356545961
path:mmu05215	Prostate cancer	99	12	0.003235	12.12121212

Abbreviations: KEGG,Kyoto Encyclopedia of Genes and Genomes; N, number of pathway genes in total; DE, number of differentially expressed genes; P.DE, p value of defferentially expressed genes.

Supporting Table S4. Sequences of qPCR Primers.

Genes	Forward primer sequences (5'-3')	Reverse primer sequences (5'-3')
18s rRNA	CGGCTACCACATCCAAGGAA	GCTGGAATTACCGCGGCT
Cdc6 (Mouse)	TGGCATCATACAAGTTTGTGTGG	CAGGCTGGACGTTTCTAAGTTTT
Mcm4 (Mouse)	GAGGAAAGCAGGTCGTCACC	AGGGCTGGAAAACAAGGCATT
E2f1 (Mouse)	CTCGACTCCTCGCAGATCG	GATCCAGCCTCCGTTTCACC
Skp2 (Mouse)	CCTCCAAGGAAACGAGTCAAG	CAGGAGACACCTGGAAAGTTC

Supporting Table S5. List of antibodies used for Western blot analysis.

Antibody	Catalogue No.	Company	Concentration
4EBP1	9644	Cell Signaling Technology	1:2000
p-4EBP1 (Ser65)	9451	Cell Signaling Technology	1:2000
ACC	3676	Cell Signaling Technology	1:1000
AKT	9272	Cell Signaling Technology	1:1000
p-AKT (Ser473)	4060	Cell Signaling Technology	1:1000
p-AKT (Thr308)	9275	Cell Signaling Technology	1:1000
AMPK	5831	Cell Signaling Technology	1:1000
p-AMPK	2535	Cell Signaling Technology	1:1000
β-Catenin	BD610153	BD Biosciences	1:2000
CCNA	sc-751	Santa Cruz Biotechnology	1:500
CCNB1	sc-245	Santa Cruz Biotechnology	1:250
CCND1	ab134175	Abcam	1:10000
CCNE	sc-481	Santa Cruz Biotechnology	1:200
Cleaved Caspase 3	9664	Cell Signaling Technology	1:1000
Cleaved Caspase 7	8438	Cell Signaling Technology	1:1000
Cleaved PARP	5625	Cell Signaling Technology	1:1000
c-MET	71-8000	Invitrogen	1:400
p-MET ((Tyr1234/1235))	3077	Cell Signaling Technology	1:200
c-MYC	Ab32072	Abcam	1:10000
ERK1/2	9102	Cell Signaling Technology	1:1000
p-ERK1/2 (Thr202/Tyr204)	4370	Cell Signaling Technology	1:1000
FASN	3180	Cell Signaling Technology	1:2000
GAPDH	MAB374	EMD Millipore	1:5000
HA-tag	2367	Cell Signaling Technology	1:1000
Hexokinase 2	2867	Cell Signaling Technology	1:1000
HIF-1α	14179	Cell Signaling Technology	1:500
HMGCR	ab174830	Abcam	1:10000
LDHA/LDHC	3558	Cell Signaling Technology	1:1000
LPL	ab21356	Abcam	1:1000
mTOR	2983	Cell Signaling Technology	1:1000
p-mTOR (Ser2481)	2974	Cell Signaling Technology	1:1000
p16	ab51243	Abcam	1:200
p21	556430	BD Biosciences	1:200
p27	610242	BD Biosciences	1:1000
p53	sc-126	Santa Cruz Biotechnology	1:200

PCNA	2856	Cell Signaling Technology	1:2000
PFKP	8164	Cell Signaling Technology	1:1000
PKM1	7067	Cell Signaling Technology	1:1000
PKM2	4053	Cell Signaling Technology	1:1000
p-Rb (Ser780)	9307	Cell Signaling Technology	1:1000
S6RP	2217	Cell Signaling Technology	1:1000
p-S6RP (Ser235/236)	4858	Cell Signaling Technology	1:1000
SCD1	2794	Cell Signaling Technology	1:1000
Survivin	2808	Cell Signaling Technology	1:1000

Supporting Table S6. List of antibodies used for immunohistochemistry.

Antibody	Catalogue No.	Company	Concentration
ACC	3676	Cell Signaling Technology	1:100
CD34	ab81289	Abcam	1:2000
CD45	550539	BD Biosciences	1:50
CD8	14-0808-82	Invitrogen	1:100
CK19	ab133496	Abcam	1:500
Cleaved Caspase 3	9664	Cell Signaling Technology	1:100
c-MYC	Ab32072	Abcam	1:200
F4/80	14-4801-82	eBioscience	1:100
FASN	3180	Cell Signaling Technology	1:200
HA-tag	2367	Cell Signaling Technology	1:150
Ki67	RM-9106-S1	Thermo Fisher Scientific	1:150
MYC-tag	2278	Cell Signaling Technology	1:100
PTEN	9188	Cell Signaling Technology	1:150
SOX9	ab185230	Abcam	1:500

Supplementary Figure Legends

Fig. S1. Comparisons of liver panel and lipid panel between the vehicle and TVB3664 treated *FVB/N* mice. (A) Study design. The ~40 weeks old *FVB/N* mice were treated with TVB3664 (N=5, 10mg/kg/d) or vehicle (N=5) through daily oral gavage. One treatment cycle includes 6 consecutive dosing days and 1 day of washout. Mice were scarified after 3 cycles of treatment for the following analysis. **(B)** Comparisons of liver panel and lipid panel between the vehicle (VEH) and TVB3664 (TVB) treated FVB/N mice (N=5 /group). Abbreviations: ALT, alanine aminotransferase; AST, aspartate aminotransferase; TP, total protein; ALB, albumin; TBIL, total bilirubin; DBIL, direct bilirubin; HDLC, high-density lipoprotein cholesterol; LDL, low-density lipoprotein. NS, no significance. Mean ± SD; Mann-Whitney test.

Fig. S2. Representative images of macroscopic views and H&E staining of the AKT induced hepatic steatosis model in the *Fasn*$^{flox/flox}$ conditional knockout mice. Macroscopically, livers from vehicle-treated AKT/pCMV mice were paler than TVB3664 treated AKT/pCMV livers and vehicle-treated AKT/Cre livers but did not show any appreciable neoplastic alteration at the time of sacrifice (4 w.p.i). At the histopathological level, AKT/pCMV mouse livers displayed the presence of multiple enlarged cells, owing to lipid accumulation. These characteristic hepatocytes were absent or very limited in number in the AKT/pCMV livers treated with TVB3664 and in AKT/Cre mice. Scale bars: 500μm for 40X, 100μm for 200X.

Fig. S3. Histological features of AKT induced hepatic steatosis model in the *Fasn*$^{flox/flox}$ conditional knockout mice. (A) Representative images of HA-AKT, FASN, ACC, and Ki67 staining in the three groups. Red arrows indicated FASN negative hepatocytes in the AKT/Cre injected *Fasn*$^{flox/flox}$ mice. Blue arrows indicated Ki67 positive cells. Scale bars: 500μm for 40X

(main images), 100μm for 200X (insets). **(B, C)** Comparisons of the percentages of HA-tag positive area (B) and Ki67 positive cells (C) in the three groups. **** $P < 0.0001$; NS, no significance.

Fig. S4. Analysis of triglyceride metabolism in the AKT induced hepatic steatosis model in the *Fasn*$^{flox/flox}$ conditional knockout mice. (A, B) Comparison of hepatic triglyceride levels in the vehicle-treated AKT/pCMV (VEH) livers, TVB3664 treated AKT/pCMV (TVB) livers and vehicle-treated AKT/Cre livers (CRE) in the *Fasn*$^{flox/flox}$ conditional knockout mice at 1 week post-injection (w.p.i., pre-treatment; [A]) and 4 w.p.i (treatment end-point; [B]). * $P < 0.05$; ** $P < 0.01$; NS, no significance. Mean ± SD; One-way ANOVA test.

Fig. S5. Macroscopic view of the sgPTEN/c-MET livers in the three groups. Liver weight is shown at the bottom of each picture.

Fig. S6. Analysis of cholesterol metabolism in the TVB3664 or Vehicle treated sgPTEN/c-MET mouse HCCs. (A,B) Hepatic cholesterol (TC), cholesteryl ester (CE), and free cholesterol (FC) levels in the sgPTEN/c-MET tumors (A) and surrounding tissues (B). * $P < 0.05$; ** $P < 0.01$; NS, no significance. Abbreviations: VEH, Vehicle; TVB, TVB3664.

Fig. S7. Effects of TVB3664 on the sgPTEN/c-MET mouse HCCs. (A-D) Analysis of fatty acid metabolism-related proteins (A), PI3K/AKT signaling pathway (B), cell cycle and apoptosis-related proteins (C), and other potential TVB3664 targets (D). GAPDH was used as the loading control. Abbreviations: FVB, *FVB/N* wild-type normal liver; PRE, pretreated sgPTEN/c-MET

tumors; VEH, Vehicle-treated sgPTEN/c-MET tumors; TVB, TVB3664-treated sgPTEN/c-MET tumors.

Fig. S8. Effects of TVB3664 on sgPTEN/c-MET-driven hepatocarcinogenesis. (A, B) The results of Western blot analysis in Fig. S7A and Fig. S7B were quantified to analyze fatty acid metabolism-related proteins (A) and PI3K/AKT signaling pathway (B). $P < 0.05$ (a) vs. FVB; (b) vs. PRE; (c) vs. VEH. Abbreviations: FVB, *FVB/N* wild-type normal liver; PRE, pretreatment; VEH, Vehicle; TVB, TVB3664.

Fig. S9. Effects of TVB3664 on the sgPTEN/c-MET mouse HCCs. (A, B) The results of Western blot analysis in Fig. S7C and Fig.S7D were quantified to analyze cell cycle and apoptosis-related proteins (A), and other potential TVB3664 targets (B). $P < 0.05$ (a) vs. FVB; (b) vs. PRE; (c) vs. VEH. Abbreviations: FVB, *FVB/N* wild-type normal liver; PRE, pretreatment; VEH, Vehicle; TVB, TVB3664.

Fig. S10. TVB3664 does not affect FASN and ACC expression in the sgPTEN/c-MET murine HCC lesions. Representative images of FASN and acetyl-CoA carboxylase (ACC) staining. Scale bars: 100μm.

Fig. S11. TVB3664 treatment inhibits the growth of AKT/NRAS mouse HCCs. (A) Study design. *FVB/N* mice were hydrodynamically injected with AKT/NRAS/SB. Mice were treated with vehicle or TVB3664 at two weeks after injection for three weeks. **(B)** Survival curve showing that TVB3664 effectively inhibits the growth of AKT/NRAS tumors. Kaplan–Meier method and log-rank

test were applied, *p*=0.0159. **(C)** Liver weight in each group at the time of sacrifice. **(D)** Representative images of HE, HA-tag (AKT), Ki67 staining. **(E, F)** Comparison of Ki67 (E) and SOX9 (F) positive cells percentages in the two groups. **(G)** Representative images of CK19, SOX9, FASN, and ACC staining. Scale bars: 200μm for 100X (main images), 100μm for 200X (insets).

Fig. S12. Fatty acid uptake of human HCC cells upon oleic acid challenge. (A-C) HLE (A), MHCC97H (B), and SNU449 (C) human HCC cell lines were treated with (BSA)-conjugated oleic for 24 hours, with BSA treatment as the controls. Cells were fixed and stained with Oil-Red-O after treatment. Representative images of Oil-Red-O staining in each group are presented. Scale bars: 100μm.

Fig. S13. Effects of combined cabozantinib/TVB3664 treatment on HCC. Representative Western blot analysis phosphorylated MET, AKT/mTOR pathway, MAPK pathway, proliferation, and apoptosis pathway as well as main fatty acid metabolic enzymes in MHCC97-H and HLE cell lines. GAPDH was used as the loading control. Abbreviations: D, DMSO; C, cabozantinib; T, TVB3664; C+T, cabozantinib/TVB3664.

Fig. S14. Macroscopic view of the sgPTEN/c-MET murine HCCs in the five groups. Liver weight is shown at the bottom of each picture. Abbreviation: C+T, cabozantinib/TVB3664.

Fig. S15. Representative images of H&E, FASN, and acetyl-CoA carboxylase (ACC) staining. Scale bars: 200μm for H&E, 500μm for FASN and ACC. Abbreviation: C+T, cabozantinib/TVB3664.

Fig. S16. Effects on the angiogenesis in the five groups. Representative images of CD34 staining. Scale bars: 200μm for 100X, 100μm for 200X. Abbreviation: C+T, cabozantinib/TVB3664.

Fig. S17. Analysis of serum liver panel and lipid metabolism in the TVB3664 and/or Cabozantinib treated sgPTEN/c-MET mouse HCCs. (A, B) Results of the liver panel (A) and lipid panel (B) in the five groups. One-way ANOVA test was applied. P < 0.05 (a) vs. NL; (b) vs. PRE; (c) vs. VEH; (e) vs. TVB. Abbreviations: NL, normal liver; PRE, pretreatment; VEH, Vehicle; CAB, cabozantinib; TVB, TVB3664; C+T, cabozantinib/TVB3664. ALT, alanine aminotransferase; AST, aspartate aminotransferase; ALB, albumin; TP, total protein; CHOL, cholesterol; TRIG, triglyceride; LDLC, low-density lipoprotein cholesterol; HDLC, high-density lipoprotein cholesterol.

Fig. S18. Effects of TVB3664 on the immune environment of sgPTEN/c-MET mouse HCCs. (A) Representative images of F4/80, CD45, and CD8 staining. **(B-D)** Comparison of percentages of F4/80 positive areas (B), CD45 positive cells, and CD8 positive cells in the three groups. * P < 0.05; ** P < 0.01; *** P < 0.001; **** P < 0.0001; NS, no significance. Scale bars: 200μm. Abbreviations: PRE, pretreatment; VEH, Vehicle, TVB, TVB3664.

Fig. S19. TVB3664 combined with anti-PDL1 antibody administration shows limited anti-tumor effects on sgPTEN/c-MET mouse HCCs. (A) Study design. *FVB/N* mice were hydrodynamically injected with sgPTEN/c-MET/SB. At ten weeks after injection, one group of mice (N=5) was sacrificed, and liver tissues were harvested as pretreatment. Other mice were

randomly assigned into the vehicle (VEH; N=5), anti-PDL1 (PD-L1; N=5), TVB3664 (TVB; N=5), or anti-PDL1 and TVB3664 combinational (Combo; N=6) treated groups. Mice were treated for three weeks and then were sacrificed. **(B)** Liver weight in the five groups. **(C)** Representative images of H&E and PTEN staining. Scale bars: 200μm for H&E and 100μm for PTEN. **(D, E)** Comparison of percentages of Ki67 positive cells (D) and PTEN negative areas (E) in the five groups.

Fig. S20. Differentially expressed genes in the TVB3664 and cabozantinib combinational treatment of the sgPTEN/c-MET mouse HCCs. (A) Top 50 differentially expressed genes (DEG) in the TVB3664 (TVB; N=4), cabozantinib (CAB; N=4), and combinational (COM; N=4) treated groups. In addition, vehicle-treated control (VEH; N=4) and untreated (FVB; N=3) groups were included. **(B)** Analysis of common and distinct canonical pathways by Ingenuity Pathway Analysis. **(C)** Inhibited upstream regulators of DEG in the COM group. Values indicate the *z*-scores of predicted states in the COM, CAB, and TVB groups for the indicated upstream regulators. **(D)** The Vegf-regulated and **(E)** the HGF-regulated networks in the COM group are depicted. Abbreviations: n.d., not detected; FVB, *FVB/N* wildtype normal liver; VEH, Vehicle, CAB, cabozantinib; TVB, TVB3664; C+T, cabozantinib/TVB3664.

Fig. S21. Effects of TVB3664 and cabozantinib combinational treatment on the sgPTEN/c-MET mouse HCCs. (A) Numbers of overlapping upregulated genes in the Cabozantinib (CAB), TVB3664 (TVB), and Cabozantinib and TVB3664 (COM) treated samples as compared to the vehicle-treated samples. **(B-D)** KEGG analysis of upregulated genes in the TVB3664 (B), Cabozantinib (C), and Cabozantinib and TVB3664 (D) combinational treated samples as compared to the vehicle-treated samples.

Fig. S22. TVB3664 in combination with Cabozantinib reduces cell cycle-related gene expression in the sgPTEN/c-MET mouse HCCs. Heatmap showing the levels of major cell cycle-related genes in the normal liver (FVB), vehicle-treated tumors (VEH), and TVB3664/cabozantinib (COM) treated tumors.

Fig. S23. Macroscopic view of the pretreatment, vehicle-, TVB3664, cabozantinib, sorafenib, cabozantinib/TVB3664, and sorafenib/TVB3664 treated c-MYC tumors. Liver weight is shown at the bottom of each picture. Abbreviations: PRE, pretreatment; VEH, Vehicle; TVB, TVB3664; CAB, cabozantinib; SOR, sorafenib; C+T, cabozantinib/TVB3664, S+T, sorafenib/TVB3664.

Fig. S24. Representative images of H&E staining in the pretreatment (PRE), vehicle- (VEH), TVB3664 (TVB), cabozantinib (CAB), sorafenib (SOR), cabozantinib/TVB3664 (C+ T), and sorafenib/TVB3664 (S+ T) treated c-MYC tumors. Scale bars: 500μm for 40X (main images), 100μm for 200X (insets).

Fig. S25. Representative images of c-MYC staining in the pretreatment (PRE), vehicle- (VEH), TVB3664 (TVB), cabozantinib (CAB), sorafenib (SOR), cabozantinib/TVB3664 (C+ T), and sorafenib/TVB3664 (S+ T) treated c-MYC tumors. Scale bars: 500μm for 40X (main images), 100μm for 200X (insets).

Fig. S26. Representative images of Ki67 staining in the pretreatment (PRE), vehicle- (VEH), TVB3664 (TVB), cabozantinib (CAB), sorafenib (SOR), cabozantinib/TVB3664 (C+ T), and sorafenib/TVB3664 (S+ T) treated c-MYC tumors. Scale bars: 100 μm.

Fig. S27. Representative images of cleaved caspase-3 staining in the pretreatment (PRE), vehicle- (VEH), TVB3664 (TVB), cabozantinib (CAB), sorafenib (SOR), cabozantinib/TVB3664 (C+ T), and sorafenib/TVB3664 (S+ T) treated c-MYC tumors. Scale bars: 100 μm.

Fig. S28. Representative images of CD34 staining in the pretreatment (PRE), vehicle- (VEH), TVB3664 (TVB), cabozantinib (CAB), sorafenib (SOR), cabozantinib/TVB3664 (C+ T), and sorafenib/TVB3664 (S+ T) treated c-MYC tumors. Scale bars: 100 μm.

Fig. S29. Analysis of hepatic triglyceride and cholesterol levels in the TVB3664 treated c-MYC mouse HCCs. (A) Hepatic triglyceride levels in the c-MYC tumors (T) and surrounding liver tissues (SL). **(B, C)** Hepatic cholesterol (TC), cholesteryl ester (CE), and free cholesterol (FC) levels in the c-MYC tumors (B) and surrounding tissues (C). * $P < 0.05$; ** $P < 0.01$; NS, no significance. Abbreviations: VEH, Vehicle; TVB, TVB3664.

Fig. S30. Effects of TVB3664 on the c-MYC mouse HCC lesions. (A-D) Analysis of fatty acid metabolism-related proteins (A), PI3K/AKT signaling pathway (B), cell cycle and apoptosis-related proteins (C), and other potential TVB3664 targets (D). GAPDH was used as the loading

control. Abbreviations: FVB, *FVB/N* wild-type normal liver; PRE, pretreated c-MYC tumors; VEH, Vehicle-treated c-MYC tumors; TVB, TVB3664-treated c-MYC tumors.

Fig. S31. Effects of TVB3664 and tyrosine kinase inhibitors treatment on the c-MYC mouse HCC lesions. (A) Analysis of PI3K/AKT signaling pathway and cell cycle-related proteins in TVB3664/cabozantinib treated c-MYC tumors. (B) Analysis of PI3K/AKT signaling pathway and cell cycle-related proteins in TVB3664/sorafenib treated c-MYC tumors. GAPDH was used as the loading control. Abbreviations: PRE, pretreatment; VEH, vehicle; TVB, TVB3664; CAB, cabozantinib; SOR, sorafenib; C+T, cabozantinib/TVB3664; S+T, sorafenib/TVB3664.

Fig. S32. Effects of TVB3664 on the β-CateninΔ90/c-MET mouse HCC lesions. (A-D) Analysis of fatty acid metabolism-related proteins (A), PI3K/AKT signaling pathway (B), cell cycle, and apoptosis-related (C) proteins. Abbreviations: FVB, *FVB/N* wild-type normal liver; PRE, pretreatment; VEH, Vehicle; TVB, TVB3664.

Fig. S33. Analysis of TVB3664 effect on the RB/E2F1 pathway. (A-C) mRNA expressions of *Cdc6, E2f1, Mcm4,* and *Skp2* in the AKT model (A), sgPTEN/c-MET model (B), and c-MYC model (C). $P < 0.05$ (a) vs. NL; (b) vs. VEH. Abbreviations: NL, normal liver; VEH, Vehicle; TVB, TVB3664.

Fig. S34. C75 and cabozantinib concomitant treatment induces growth inhibition in human HCC cell lines. (A) IC50 values of C75 and cabozantinib (same as in Fig. 3) in the MHCC97H, HLE, and SNU449 human HCC cell lines. **(B-D)** Cell viability in the DMSO, cabozantinib, C75,

and combinational treated groups with ~IC50 concentrations as indicated in MHCC97H (B), HLE (C), and SNU449 (D) human HCC cells. $P < 0.05$ (a) vs. DMSO; (b) vs. Cabozantinib; (C) vs. C75.

Fig. S35. TVB3664 has minor effects on the expression of *de novo* lipogenesis-related genes. The relative expression (in FPKM) of acetyl-CoA by ATP-citrate lyase (*Acly*), acetyl-CoA carboxylases 1 (ACC1, encoded by *Acaca*), fatty acid synthase (*Fasn*), sterol regulatory element-binding protein 1c (SREBP1c, encoded by *Srebf1*), carbohydrate-response element-binding protein (ChREBP, encoded by *Mlxipl*), liver X receptor alpha (encoded by *Nr1h3*), and liver X receptors beta (encoded by *Nr1h2*) in the sgPTEN/c-MET tumors treated with vehicle and TVB3664. Abbreviations: VEH, Vehicle; TVB, TVB3664.

Fig. S36. TVB3664 does not affect the expression of genes encoding glycolytic enzymes. The relative expression (in FPKM) of *Hk4, Pfkl, Pfkm, Pfkp, Pkm, Ldha, Ldhb, Aldoa, Pgk1* in the sgPTEN/c-MET tumors treated with vehicle and TVB3664. Abbreviations: VEH, Vehicle; TVB, TVB3664.

Fig. S37. TVB3664 does not affect the expression of genes in the fatty acid β-oxidation cycle or Foxp3. (A) The relative expression (in FPKM) of very long-chain acyl-CoA dehydrogenase (*Acadvl*), long-chain acyl-CoA dehydrogenase (*Acadl*), medium-chain acyl-CoA dehydrogenase (*Acadm*), acyl-CoA dehydrogenase 9 (*Acad9*), acyl-CoA oxidase 1 (*Acox1*), cytochrome P450 family 2 subfamily E member 1(*Cyp2e1*), mitochondrial trifunctional protein, alpha subunit (*Hadha*), mitochondrial trifunctional protein, beta subunit (*Hadhb*) and hydroxyacyl-coenzyme A dehydrogenase (*Hadh*) in the sgPTEN/c-MET tumors treated with vehicle and TVB3664. **(B)** The relative expression (in FPKM+3) of *Foxp3* in the sgPTEN/c-MET tumors

treated with vehicle and TVB3664. Abbreviations: VEH, Vehicle; TVB, TVB3664; NS, no significance.

Fig. S38. Graphical abstract. TVB3664 effectively inhibits *de novo* lipogenesis and improves NAFLD/NASH-related effects in old mice and AKT overexpressing livers. TVB3664 monotherapy showed moderate efficacy in NASH-related murine HCCs, induced by loss of PTEN and c-MET overexpression. TVB3664, in combination with cabozantinib, triggered tumor regression in this mouse HCC model. TVB3664 also improved the therapeutic efficacy of sorafenib and cabozantinib in the FASN-dependent c-MYC HCC model. However, TVB3664 had no efficacy nor synergistic effects in FASN-independent mouse HCC models.

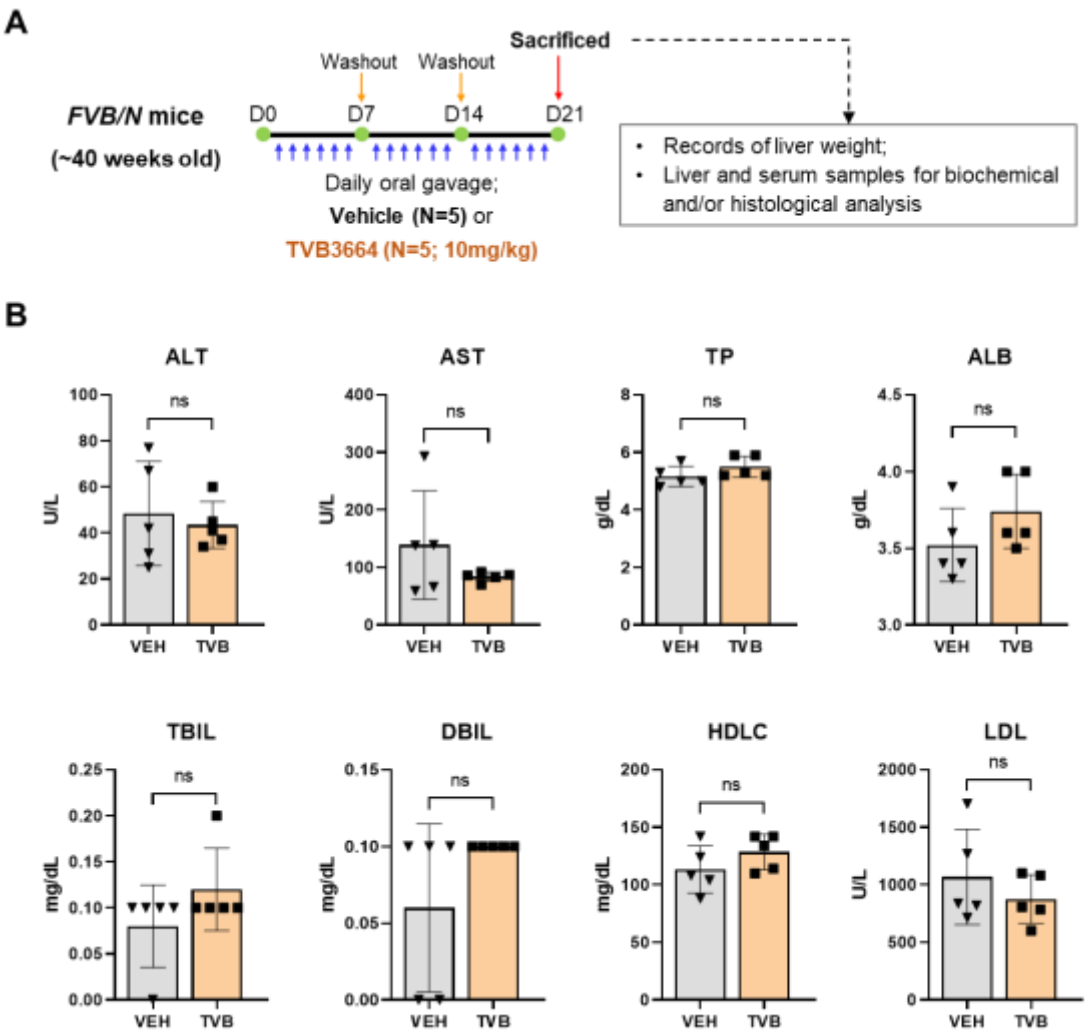

Fig. S1. Comparisons of liver panel and lipid panel between the vehicle and TVB3664 treated *FVB/N* mice. **(A)** Study design. The ~40 weeks old *FVB/N* mice were treated with TVB3664 (N=5, 10mg/kg/d) or vehicle (N=5) through daily oral gavage. One treatment cycle includes 6 consecutive dosing days and 1 day of washout. Mice were scarified after 3 cycles of treatment for the following analysis. **(B)** Comparisons of liver panel and lipid panel between the vehicle (VEH) and TVB3664 (TVB) treated FVB/N mice (N=5 /group). Abbreviations: ALT, alanine aminotransferase; AST, aspartate aminotransferase; TP, total protein; ALB, albumin; TBIL, total bilirubin; DBIL, direct bilirubin; HDLC, high-density lipoprotein cholesterol; LDL, low-density lipoprotein. NS, no significance. Mean ± SD; Mann-Whitney test.

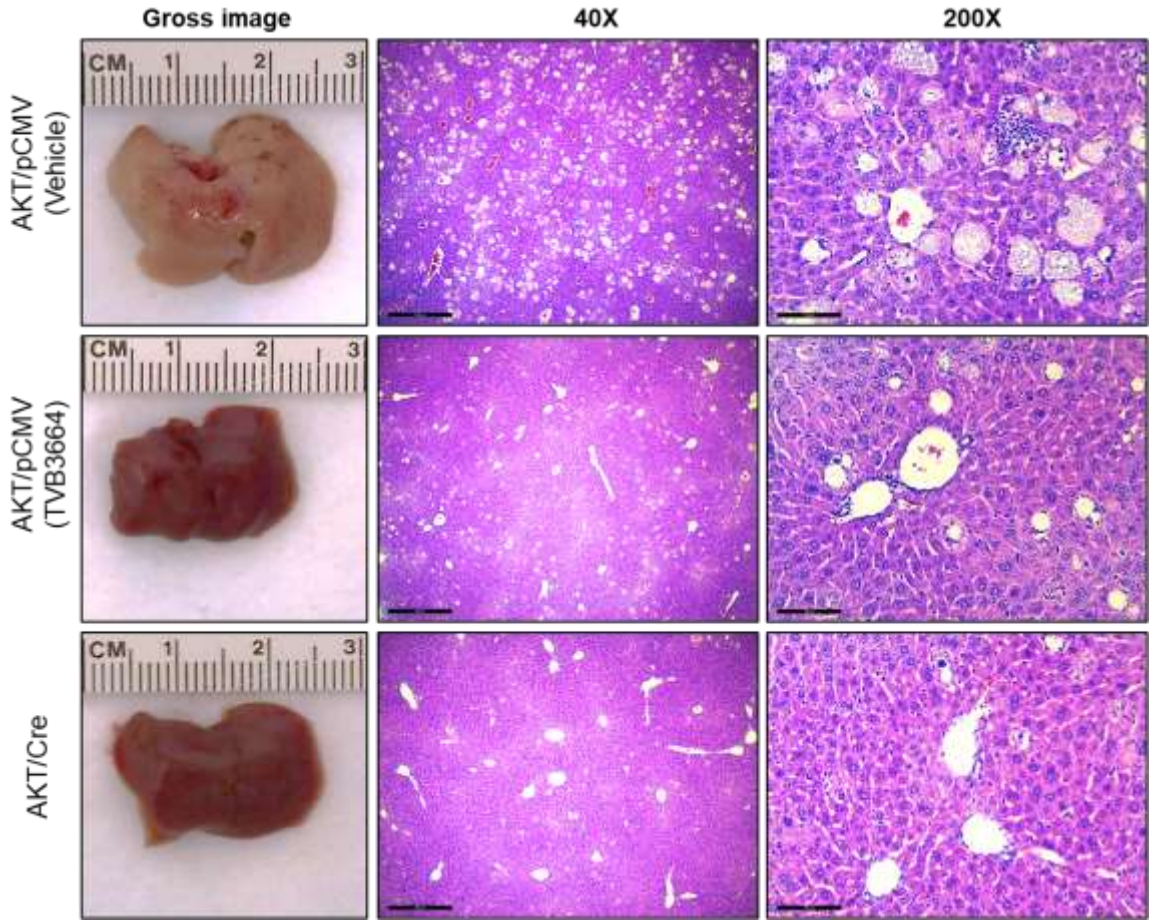

Fig. S2. Representative images of macroscopic views and H&E staining of the AKT induced hepatic steatosis model in the *Fasn*$^{flox/flox}$ conditional knockout mice. Macroscopically, livers from vehicle-treated AKT/pCMV mice were paler than TVB3664 treated AKT/pCMV livers and vehicle-treated AKT/Cre livers but did not show any appreciable neoplastic alteration at the time of sacrifice (4 w.p.i). At the histopathological level, AKT/pCMV mouse livers displayed the presence of multiple enlarged cells, owing to lipid accumulation. These characteristic hepatocytes were absent or very limited in number in the AKT/pCMV livers treated with TVB3664 and in AKT/Cre mice. Scale bars: 500μm for 40X, 100μm for 200X.

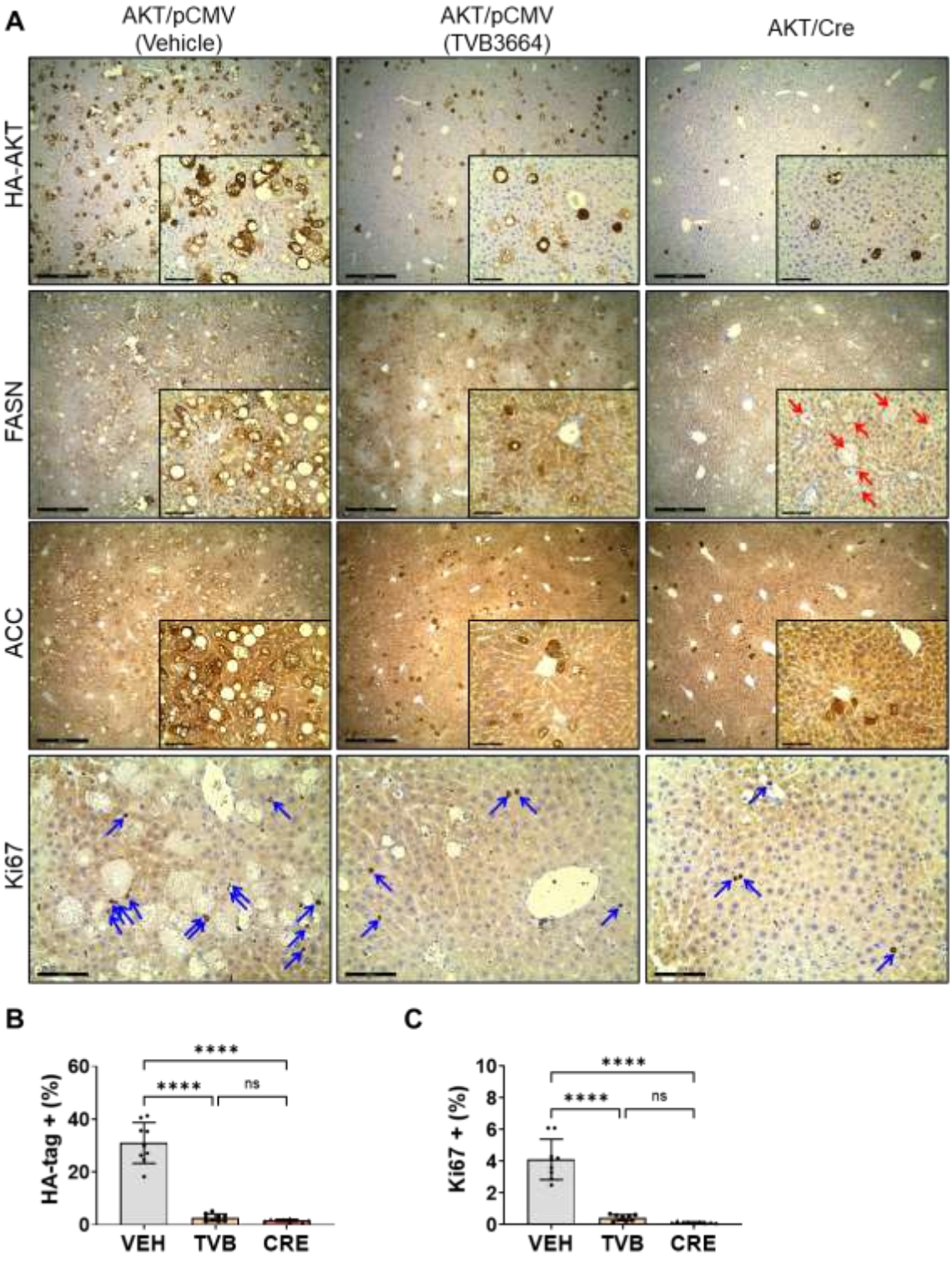

Fig. S3. Histological features of AKT induced hepatic steatosis model in the *Fasn*$^{flox/flox}$ conditional knockout mice. (A) Representative images of HA-AKT, FASN, ACC, and Ki67

staining in the three groups. Red arrows indicated FASN negative hepatocytes in the AKT/Cre injected *Fasn*$^{flox/flox}$ mice. Blue arrows indicated Ki67 positive cells. Scale bars: 500μm for 40X (main images), 100μm for 200X (insets). **(B, C)** Comparisons of the percentages of HA-tag positive area (B) and Ki67 positive cells (C) in the three groups. **** $P < 0.0001$; NS, no significance.

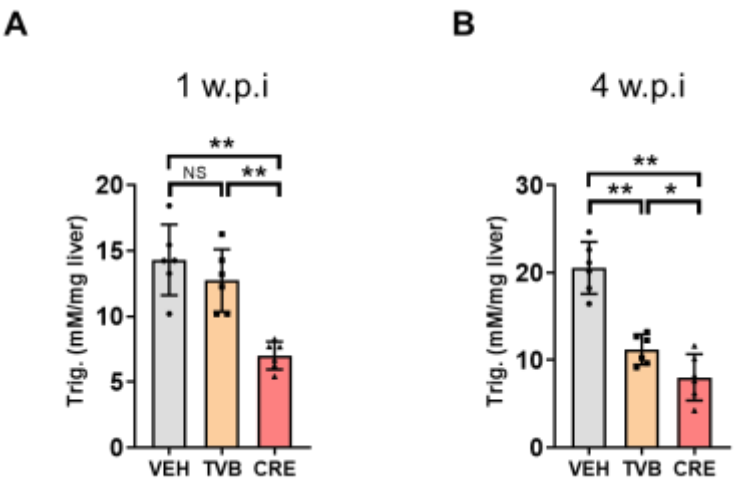

Fig. S4. Analysis of triglyceride metabolism in the AKT induced hepatic steatosis model in the *Fasn*$^{flox/flox}$ conditional knockout mice. (A, B) Comparison of hepatic triglyceride levels in the vehicle-treated AKT/pCMV (VEH) livers, TVB3664 treated AKT/pCMV (TVB) livers and vehicle-treated AKT/Cre livers (CRE) in the *Fasn*$^{flox/flox}$ conditional knockout mice at 1 week post-injection (w.p.i., pre-treatment; [A]) and 4 w.p.i (treatment end-point; [B]). * $P < 0.05$; ** $P < 0.01$; NS, no significance. Mean ± SD; One-way ANOVA test.

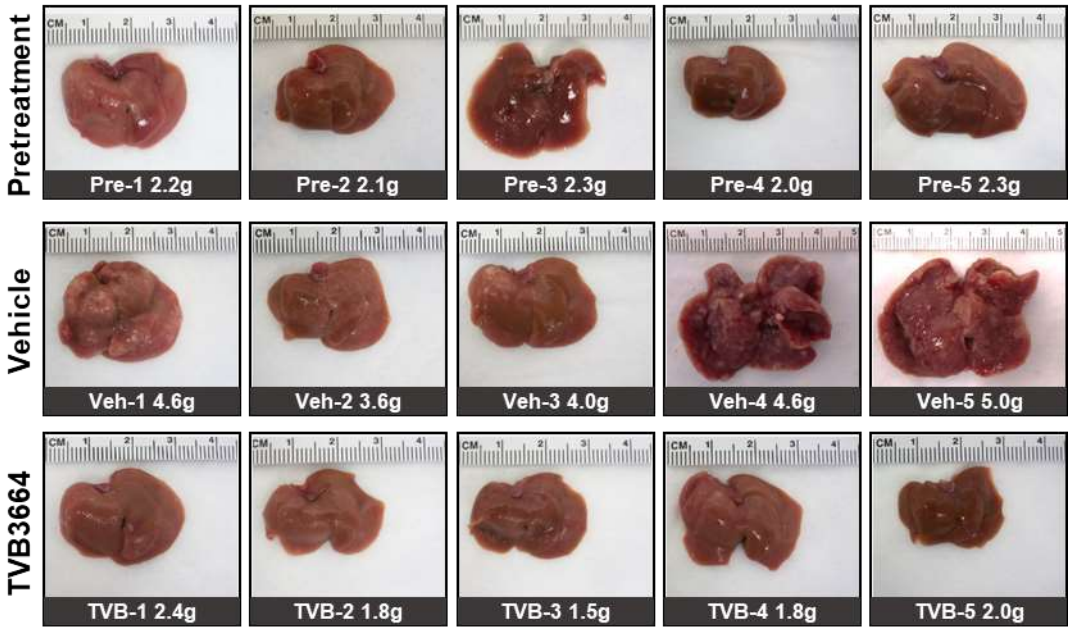

Fig. S5. Macroscopic view of the sgPTEN/c-MET livers in the three groups. Liver weight is shown at the bottom of each picture.

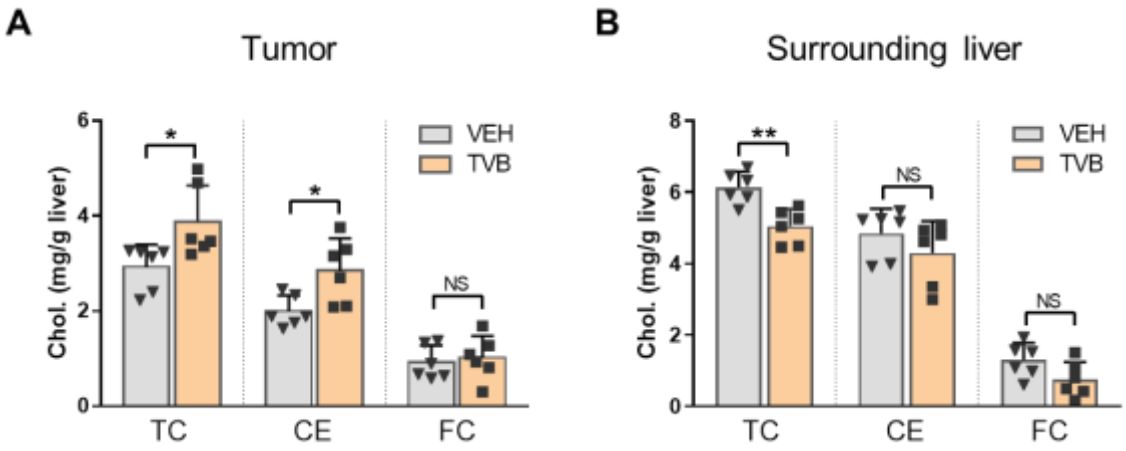

Fig. S6. Analysis of cholesterol metabolism in the TVB3664 or Vehicle treated sgPTEN/c-MET mouse HCCs. (A,B) Hepatic cholesterol (TC), cholesteryl ester (CE), and free cholesterol (FC) levels in the sgPTEN/c-MET tumors (A) and surrounding tissues (B). Mean ± SD; Mann-Whitney test. * $P < 0.05$; ** $P < 0.01$; NS, no significance. Abbreviations: VEH, Vehicle; TVB, TVB3664.

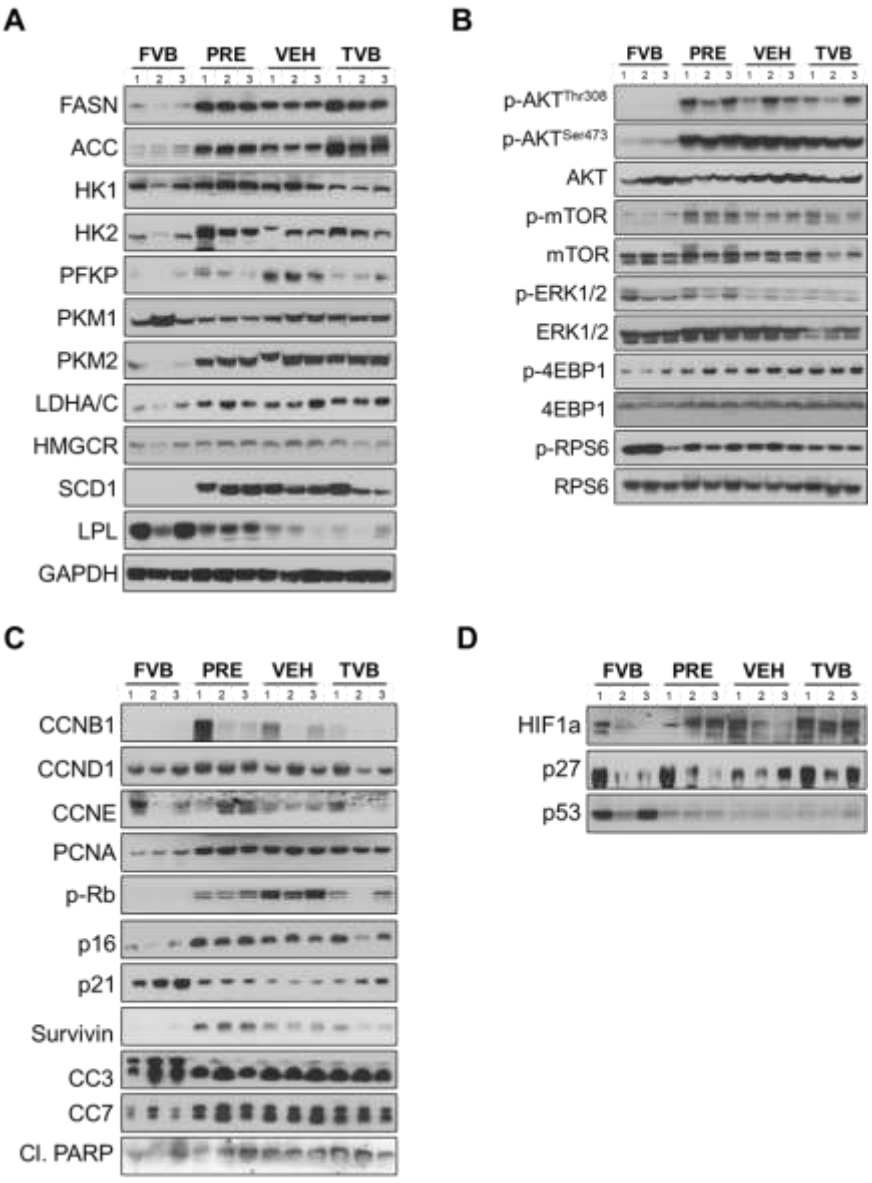

Fig. S7. Effects of TVB3664 on the sgPTEN/c-MET mouse HCCs. (A-D) Analysis of fatty acid metabolism-related proteins (A), PI3K/AKT signaling pathway (B), cell cycle and apoptosis-related proteins (C), and other potential TVB3664 targets (D). GAPDH was used as the loading control. Abbreviations: FVB, *FVB/N* wild-type normal liver; PRE, pretreated sgPTEN/c-MET tumors; VEH, Vehicle-treated sgPTEN/c-MET tumors; TVB, TVB3664-treated sgPTEN/c-MET tumors.

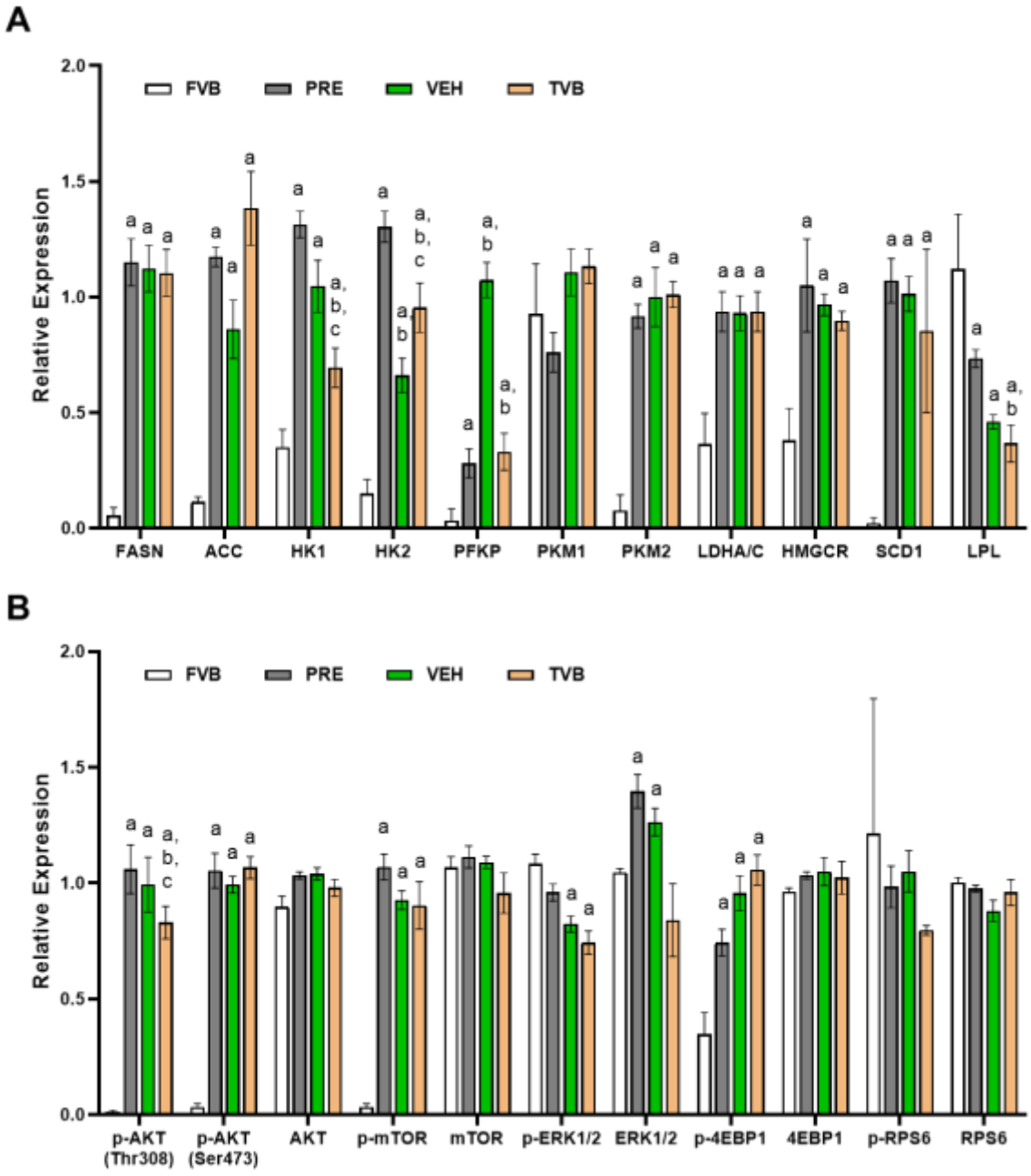

Fig. S8. Effects of TVB3664 on sgPTEN/c-MET-driven hepatocarcinogenesis. (A, B) The results of Western blot analysis in Fig. S7A and Fig. S7B were quantified to analyze fatty acid metabolism-related proteins (A) and PI3K/AKT signaling pathway (B). $P < 0.05$ (a) vs. FVB; (b) vs. PRE; (c) vs. VEH. Abbreviations: FVB, *FVB/N* wild-type normal liver; PRE, pretreatment; VEH, Vehicle; TVB, TVB3664.

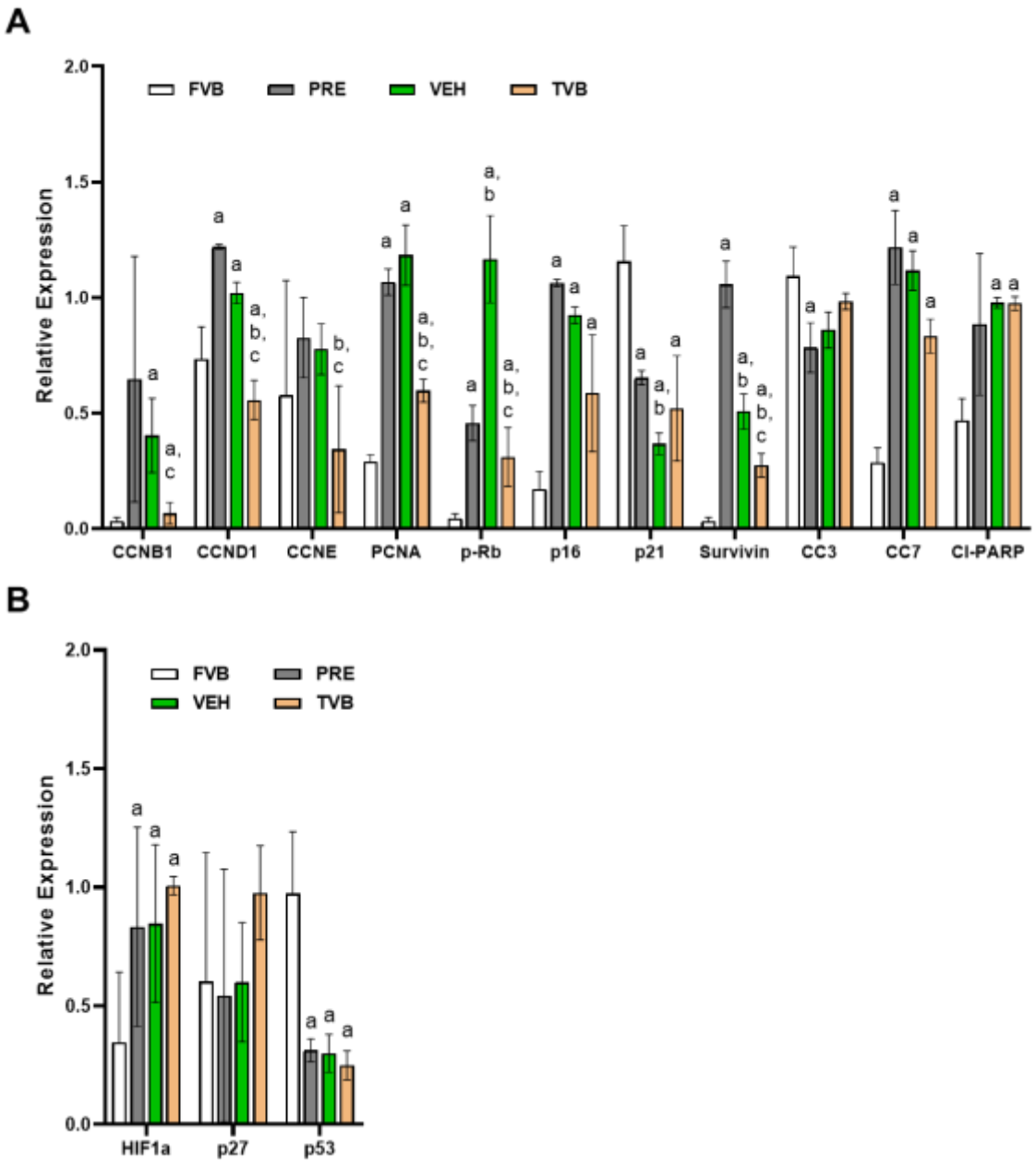

Fig. S9. Effects of TVB3664 on the sgPTEN/c-MET mouse HCCs. (A, B) The results of Western blot analysis in Fig. S7C and Fig.S7D were quantified to analyze cell cycle and apoptosis-related proteins (A), and other potential TVB3664 targets (B). $P < 0.05$ (a) vs. FVB; (b) vs. PRE; (c) vs. VEH. Abbreviations: FVB, *FVB/N* wild-type normal liver; PRE, pretreatment; VEH, Vehicle; TVB, TVB3664.

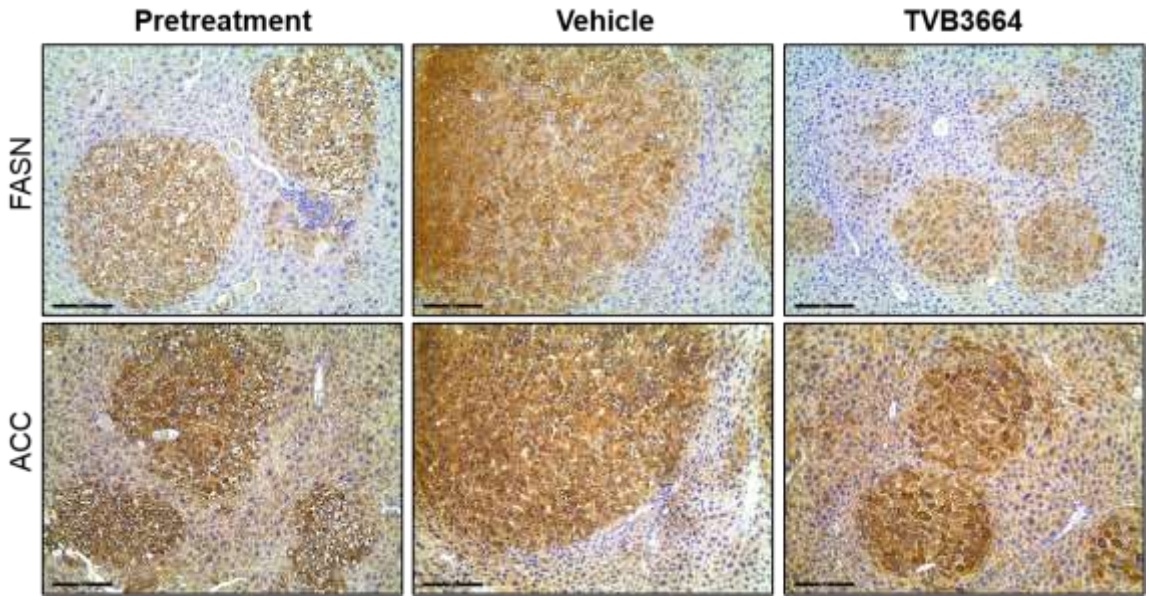

Fig. S10. TVB3664 does not affect FASN and ACC expression in the sgPTEN/c-MET murine HCC lesions. Representative images of FASN and acetyl-CoA carboxylase (ACC) staining. Scale bars: 100μm.

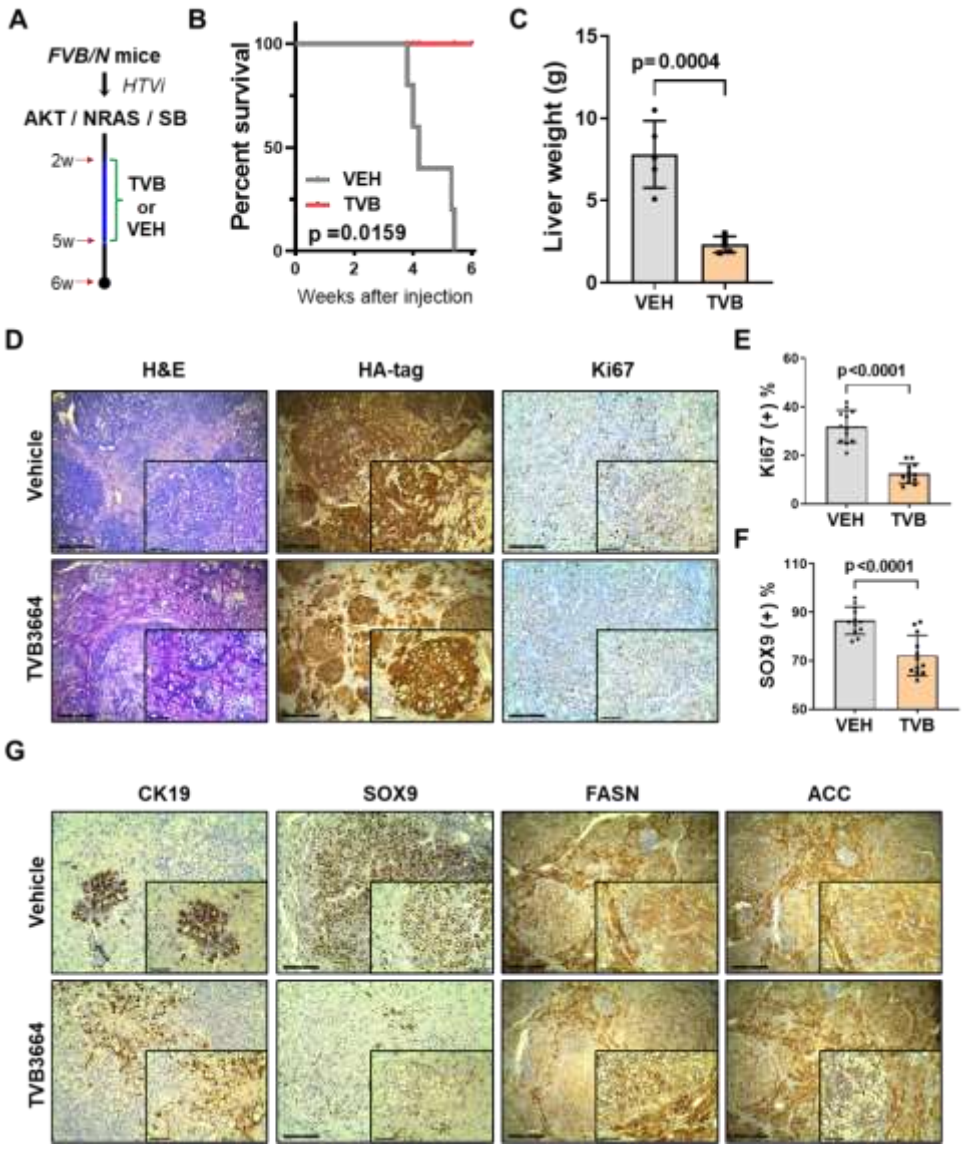

Fig. S11. TVB3664 treatment inhibits the growth of AKT/NRAS mouse HCCs. (A) Study design. *FVB/N* mice were hydrodynamically injected with AKT/NRAS/SB. Mice were treated with vehicle or TVB3664 at two weeks after injection for three weeks. **(B)** Survival curve showing that TVB3664 effectively inhibits the growth of AKT/NRAS tumors. Kaplan–Meier method and log-rank test were applied, *p*=0.0159. **(C)** Liver weight in each group at the time of sacrifice. **(D)** Representative images of HE, HA-tag (AKT), Ki67 staining. **(E, F)** Comparison of Ki67 (E) and SOX9 (F) positive cells percentages in the two groups. **(G)** Representative images of CK19, SOX9, FASN, and ACC staining. Scale bars: 200μm for 100X (main images), 100μm for 200X (insets).

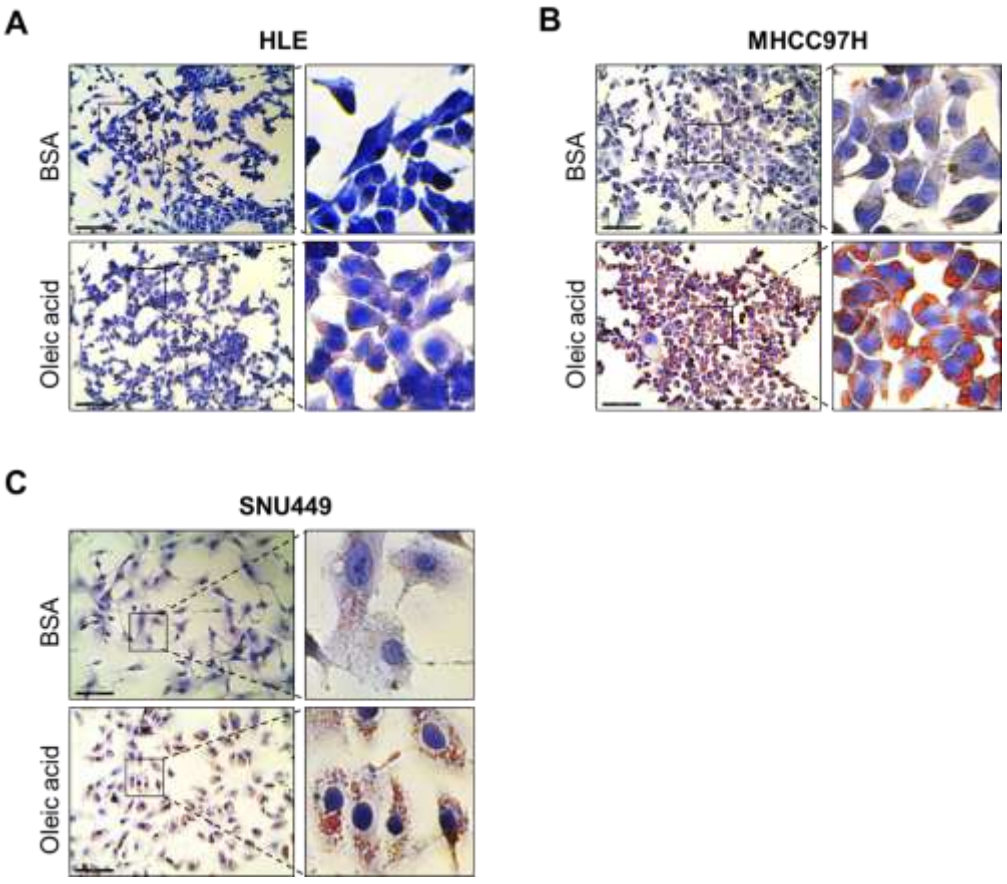

Fig. S12. Fatty acid uptake of human HCC cells upon oleic acid challenge. (A-C) HLE (A), MHCC97H (B), and SNU449 (C) human HCC cell lines were treated with (BSA)-conjugated oleic for 24 hours, with BSA treatment as the controls. Cells were fixed and stained with Oil-Red-O after treatment. Representative images of Oil-Red-O staining in each group are presented. Scale bars: 100μm.

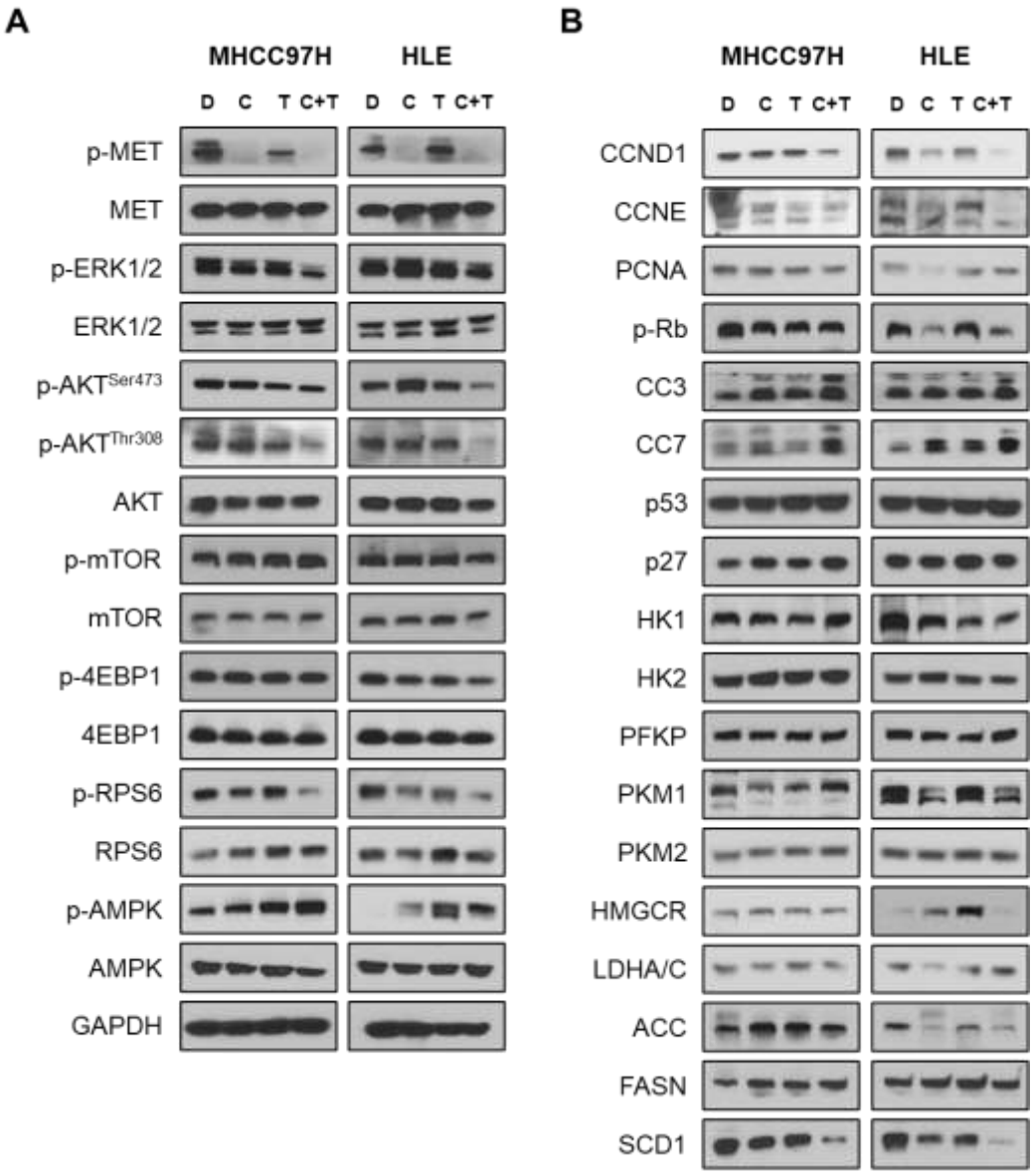

Fig. S13. Effects of combined cabozantinib/TVB3664 treatment on HCC. Representative Western blot analysis of phosphorylated MET, AKT/mTOR pathway, MAPK pathway, proliferation, and apoptosis pathway as well as main fatty acid metabolic enzymes in MHCC97-H and HLE cell lines. GAPDH was used as the loading control. Abbreviations: D, DMSO; C, cabozantinib; T, TVB3664; C+T, cabozantinib/TVB3664.

Fig. S14. Macroscopic view of the sgPTEN/c-MET murine HCCs in the five groups. Liver weight is shown at the bottom of each picture. Abbreviation: C+T, cabozantinib/TVB3664.

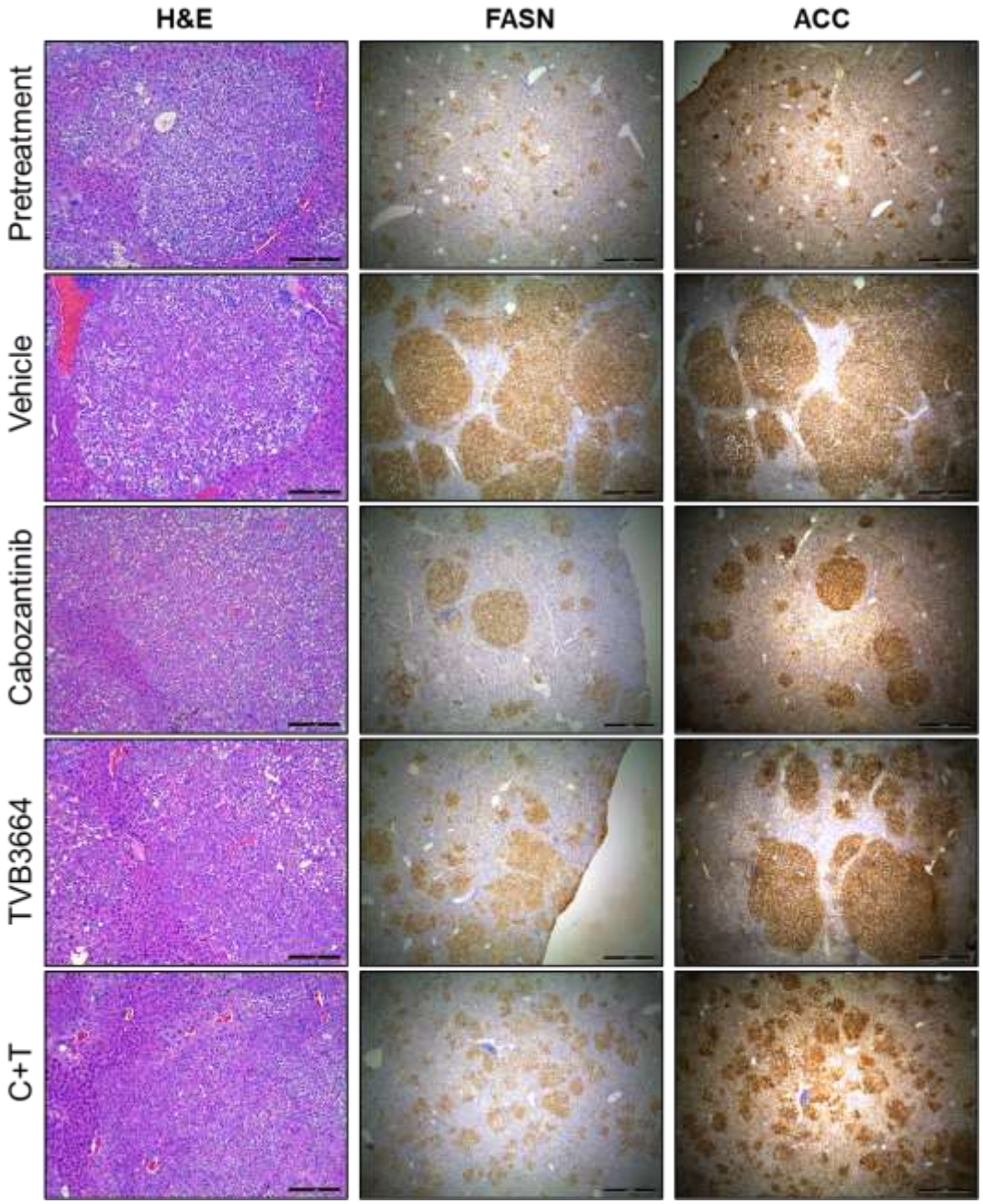

Fig. S15. Representative images of H&E, FASN, and acetyl-CoA carboxylase (ACC) staining. Scale bars: 200μm for H&E, 500μm for FASN and ACC. Abbreviation: C+T, cabozantinib/TVB3664.

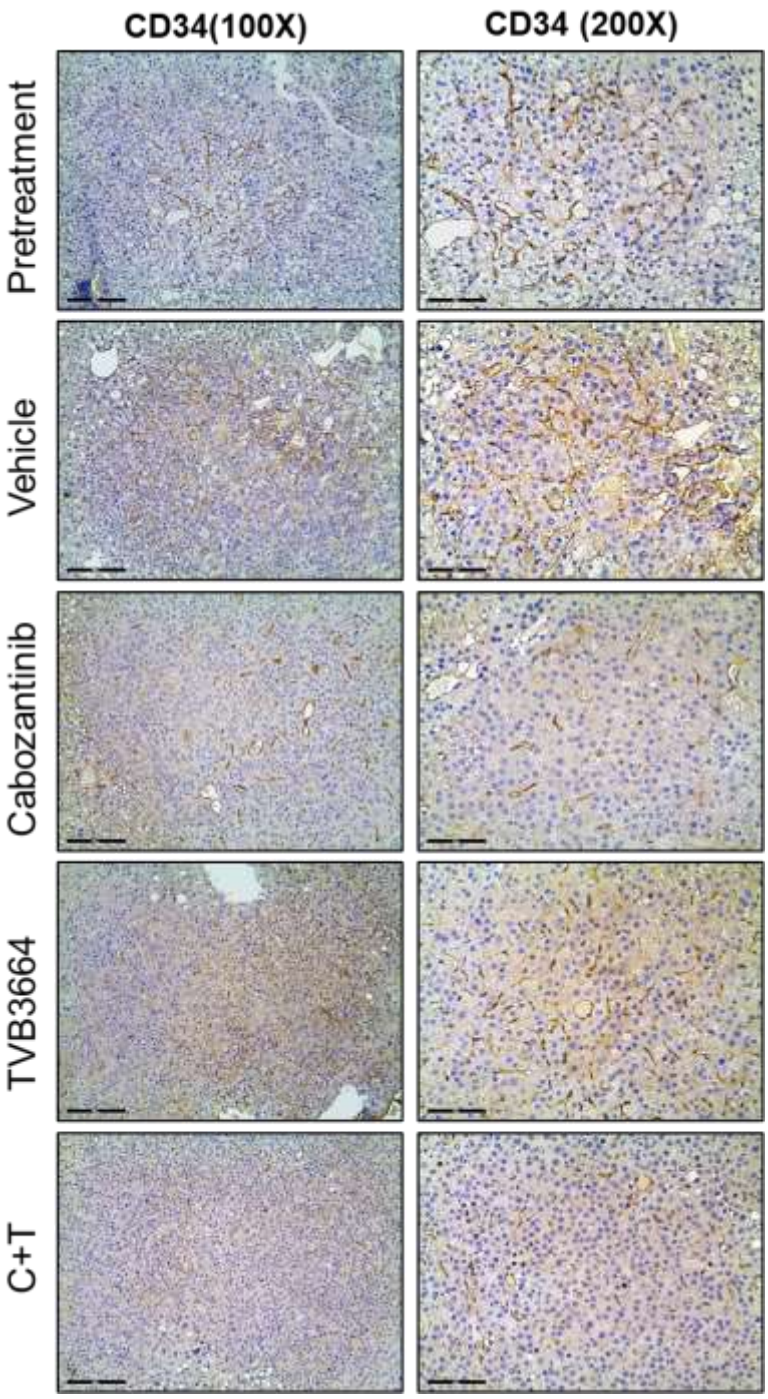

Fig. S16. Effects on the angiogenesis in the five groups. Representative images of CD34 staining. Scale bars: 200μm for 100X, 100μm for 200X. Abbreviation: C+T, cabozantinib/TVB3664.

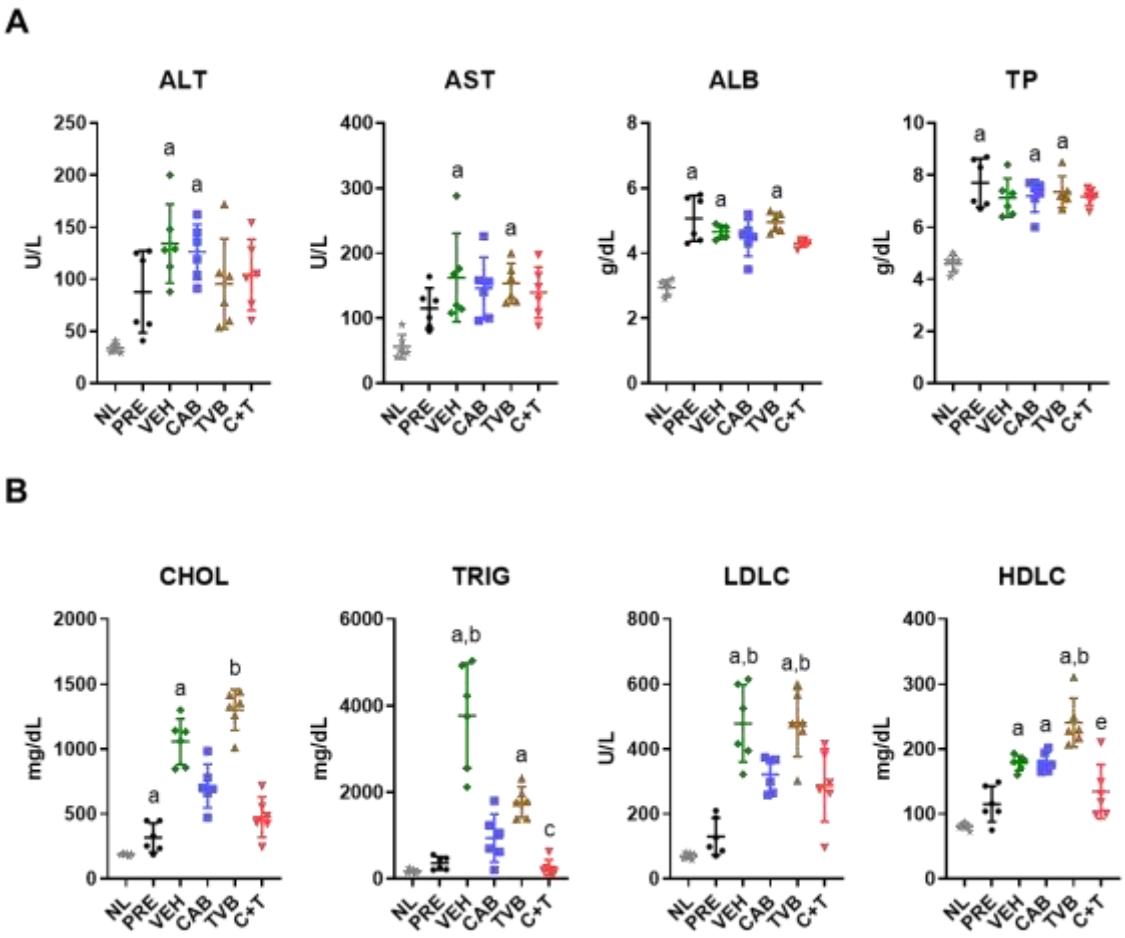

Fig. S17. Analysis of serum liver panel and lipid metabolism in the TVB3664 and/or Cabozantinib treated sgPTEN/c-MET mouse HCCs. (A, B) Results of the liver panel (A) and lipid panel (B) in the five groups. One-way ANOVA test was applied. $P < 0.05$ (a) vs. NL; (b) vs. PRE; (c) vs. VEH; (e) vs. TVB. Abbreviations: NL, normal liver; PRE, pretreatment; VEH, Vehicle; CAB, cabozantinib; TVB, TVB3664; C+T, cabozantinib/TVB3664. ALT, alanine aminotransferase; AST, aspartate aminotransferase; ALB, albumin; TP, total protein; CHOL, cholesterol; TRIG, triglyceride; LDLC, low-density lipoprotein cholesterol; HDLC, high-density lipoprotein cholesterol.

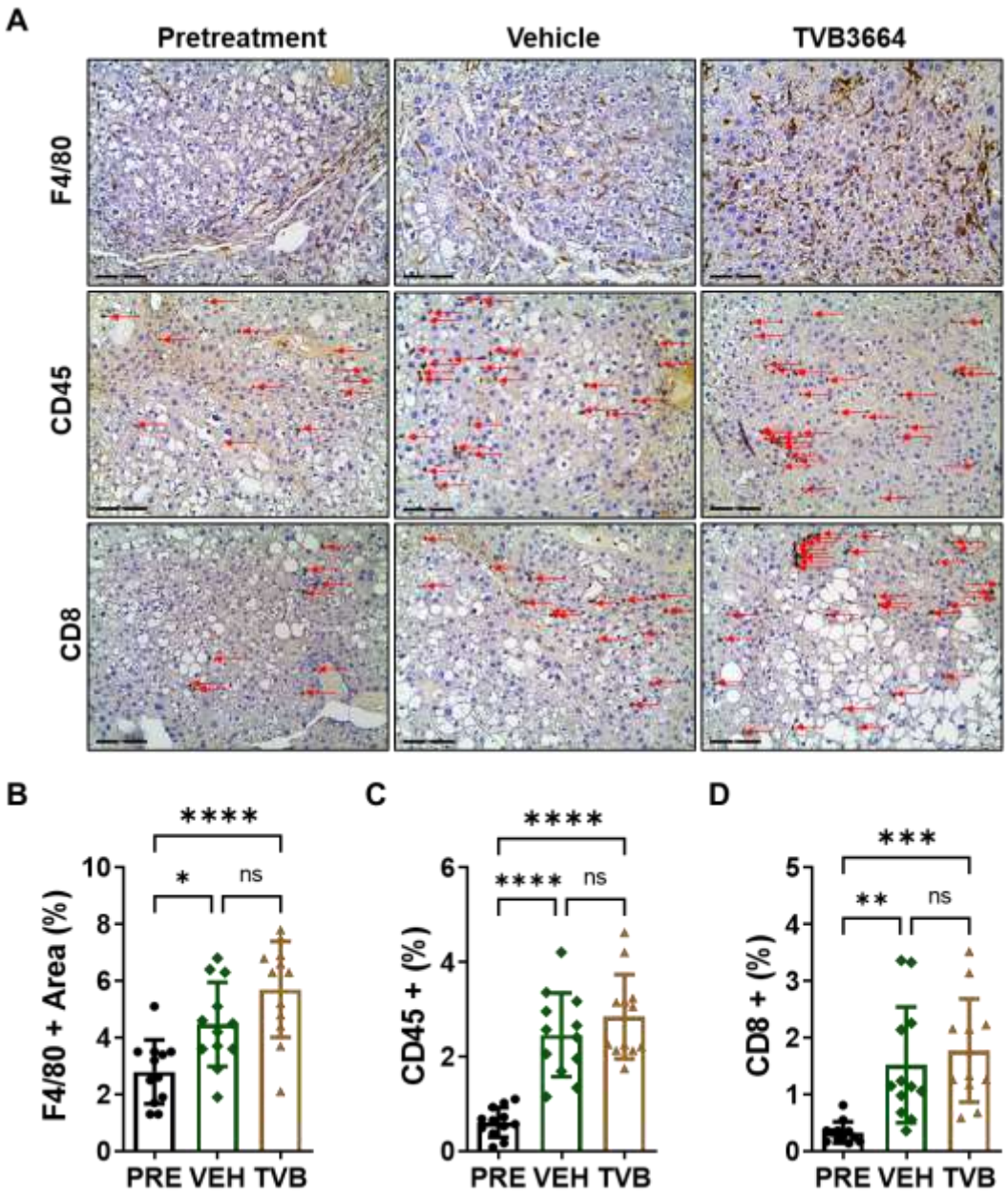

Fig. S18. Effects of TVB3664 on the immune environment of sgPTEN/c-MET mouse HCCs. **(A)** Representative images of F4/80, CD45, and CD8 staining. **(B-D)** Comparison of percentages of F4/80 positive areas (B), CD45 positive cells, and CD8 positive cells in the three groups. * $P < 0.05$; ** $P < 0.01$; *** $P < 0.001$; **** $P < 0.0001$; NS, no significance. Scale bars: 200μm. Abbreviations: PRE, pretreatment; VEH, Vehicle, TVB, TVB3664.

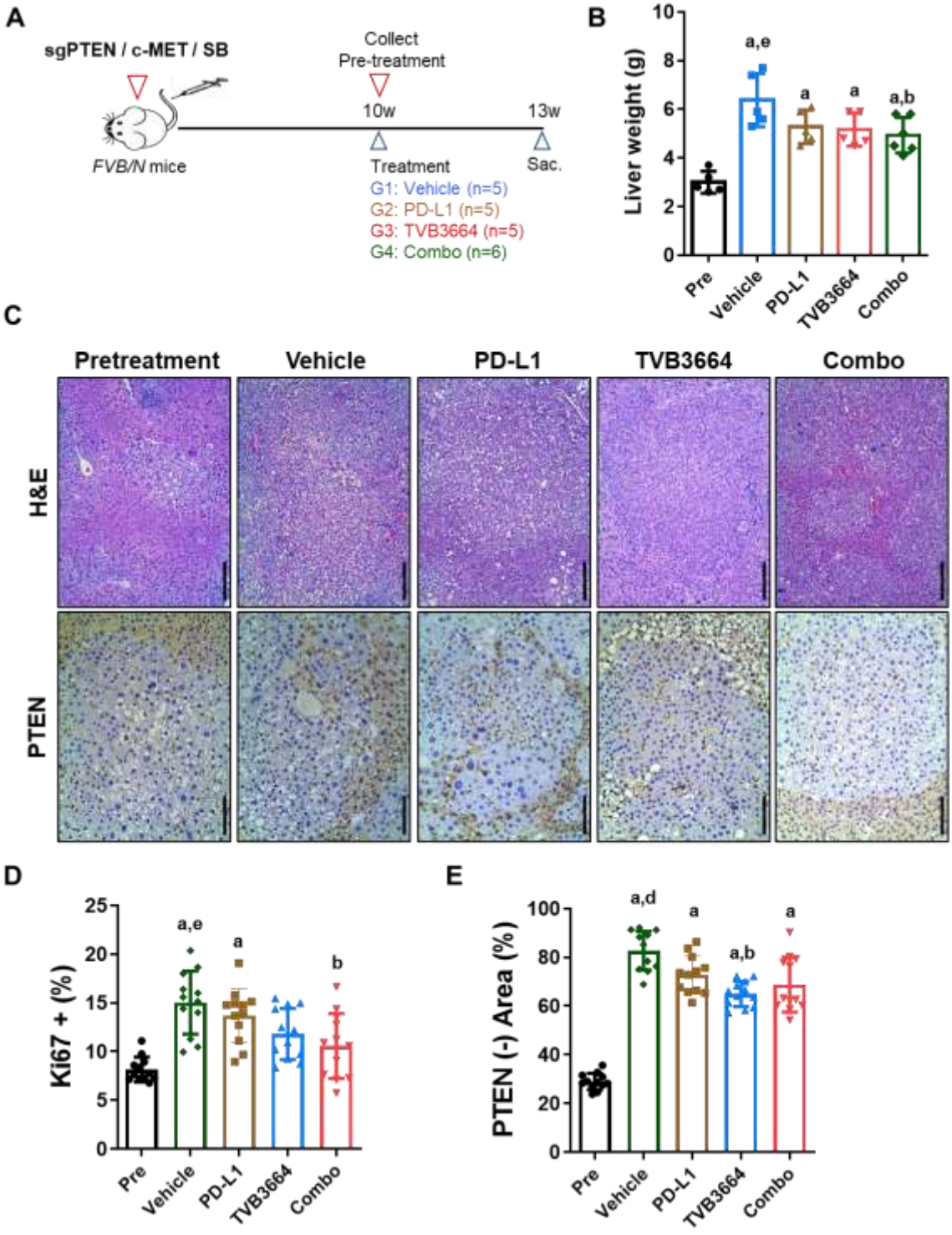

Fig. S19. TVB3664 combined with anti-PDL1 antibody administration shows limited anti-tumor effects on sgPTEN/c-MET mouse HCCs. (A) Study design. *FVB/N* mice were

hydrodynamically injected with sgPTEN/c-MET/SB. At ten weeks after injection, one group of mice (N=5) was sacrificed, and liver tissues were harvested as pretreatment. Other mice were randomly assigned into the vehicle (VEH; N=5), anti-PDL1 (PD-L1; N=5), TVB3664 (TVB; N=5), or anti-PDL1 and TVB3664 combinational (Combo; N=6) treated groups. Mice were treated for three weeks and then were sacrificed. **(B)** Liver weight in the five groups. **(C)** Representative images of H&E and PTEN staining. Scale bars: 200μm for H&E and 100μm for PTEN. **(D, E)** Comparison of percentages of Ki67 positive cells (D) and PTEN negative areas (E) in the five groups.

A

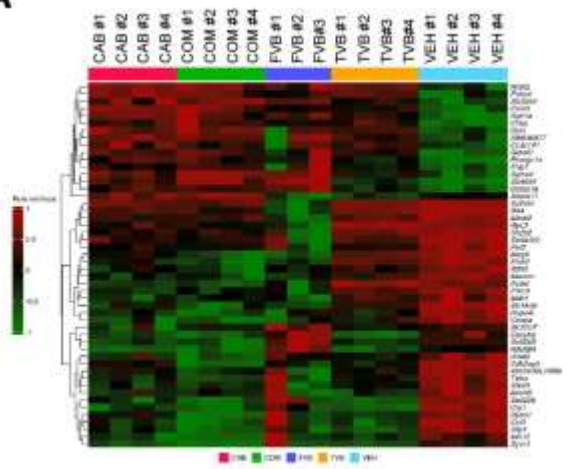

B

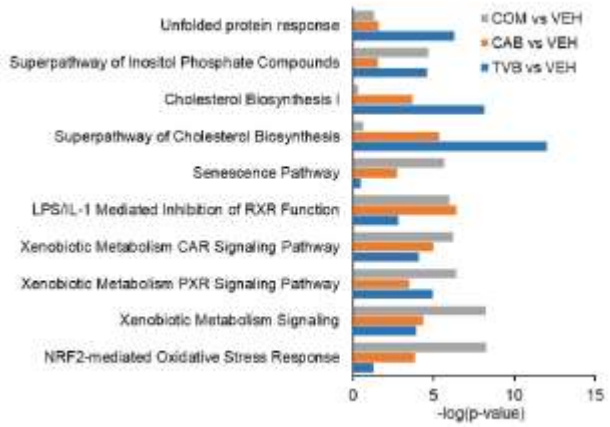

C

Upstream Regulator	Predicted State	COM	CAB	TVB
VEGF	Inhibited	-7.733	-4.781	-3.734
SP1	Inhibited	-6.183	-2.623	-2.894
HGF	Inhibited	-6.14	-2.41	n.d.
VEGFA	Inhibited	-5.532	-3.93	-2.963
NFkB (complex)	Inhibited	-4.068	-4.264	-1.644

D

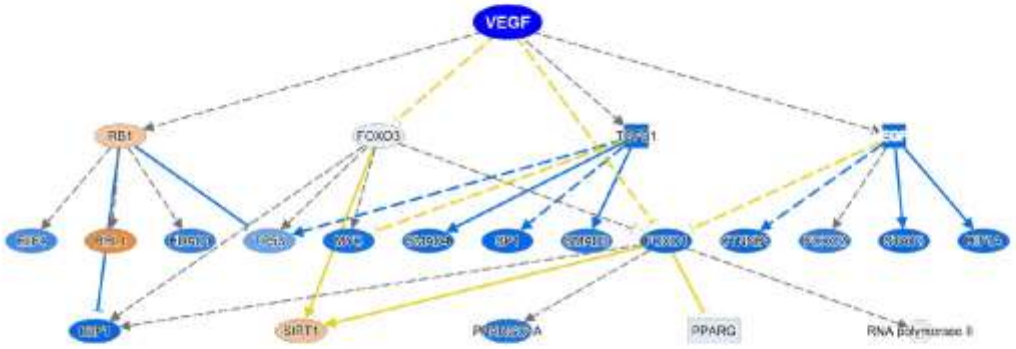

E

Fig. S20. Differentially expressed genes in the TVB3664 and cabozantinib combinational treatment of the sgPTEN/c-MET mouse HCCs. (A) Top 50 differentially expressed genes (DEG) in the TVB3664 (TVB; N=4), cabozantinib (CAB; N=4), and combinational (COM; N=4) treated groups. In addition, vehicle-treated control (VEH; N=4) and untreated (FVB; N=3) groups were included. **(B)** Analysis of common and distinct canonical pathways by Ingenuity Pathway Analysis. **(C)** Inhibited upstream regulators of DEG in the COM group. Values indicate the z-scores of predicted states in the COM, CAB, and TVB groups for the indicated upstream regulators. **(D)** The VEGF-regulated and **(E)** the HGF-regulated networks in the COM group are depicted. Abbreviations: n.d., not detected; FVB, *FVB/N* wildtype normal liver; VEH, Vehicle, CAB, cabozantinib; TVB, TVB3664; C+T, cabozantinib/TVB3664.

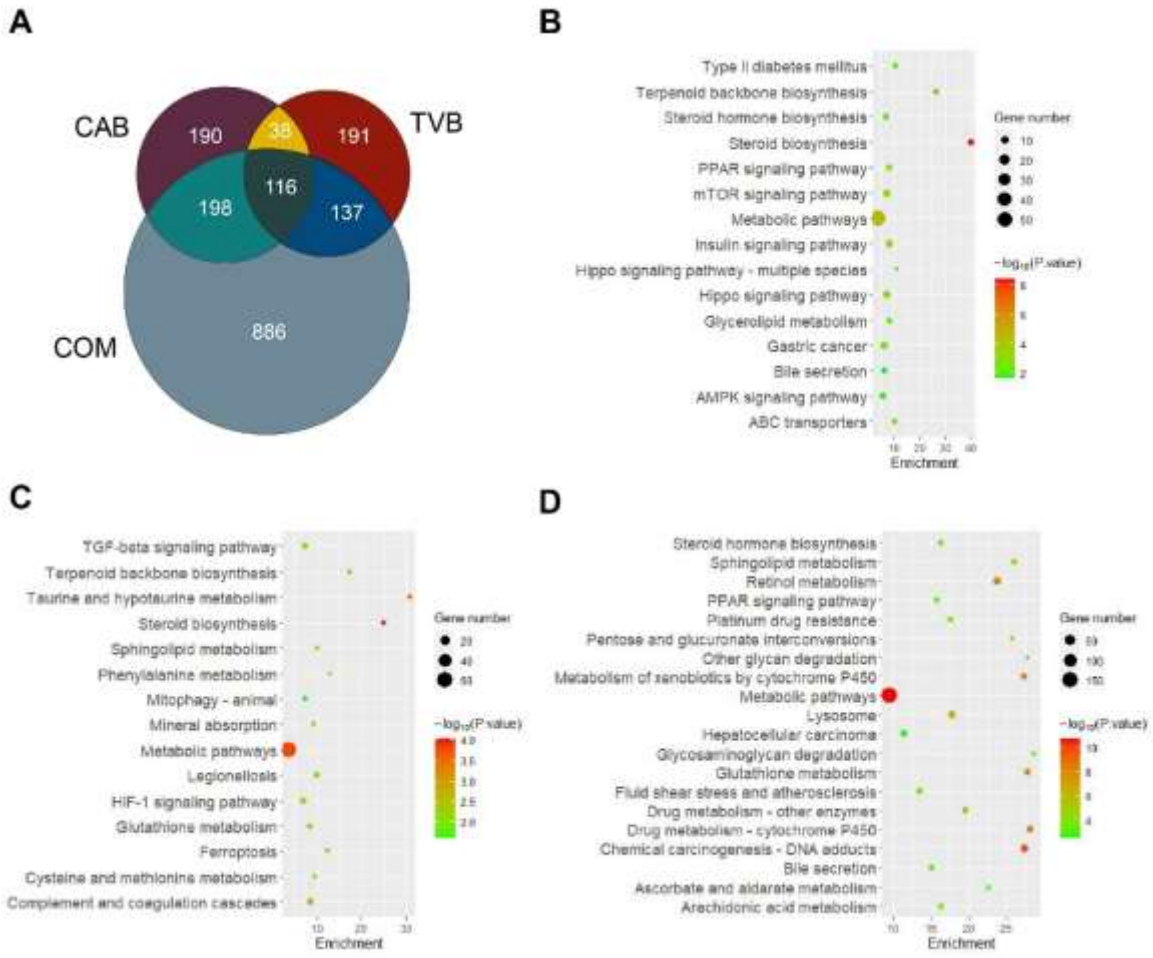

Fig. S21. Effects of TVB3664 and cabozantinib combinational treatment on the sgPTEN/c-MET mouse HCCs. (A) Numbers of overlapping upregulated genes in the Cabozantinib (CAB), TVB3664 (TVB), and Cabozantinib and TVB3664 (COM) treated samples as compared to the vehicle-treated samples. **(B-D)** KEGG analysis of upregulated genes in the TVB3664 (B), Cabozantinib (C), and Cabozantinib and TVB3664 (D) combinational treated samples as compared to the vehicle-treated samples.

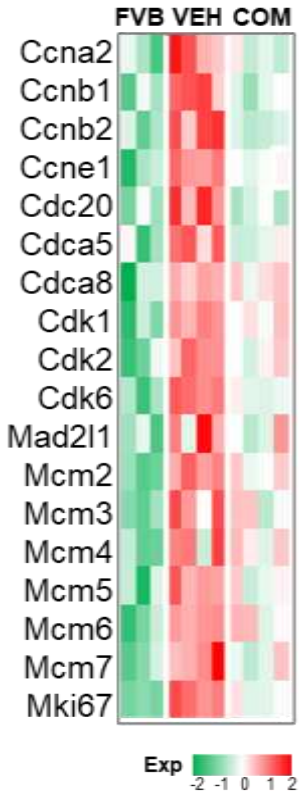

Fig. S22. TVB3664 in combination with Cabozantinib reduces cell cycle-related gene expression in the sgPTEN/c-MET mouse HCCs. Heatmap showing the levels of major cell cycle-related genes in the normal liver (FVB), vehicle-treated tumors (VEH), and TVB3664/cabozantinib (COM) treated tumors.

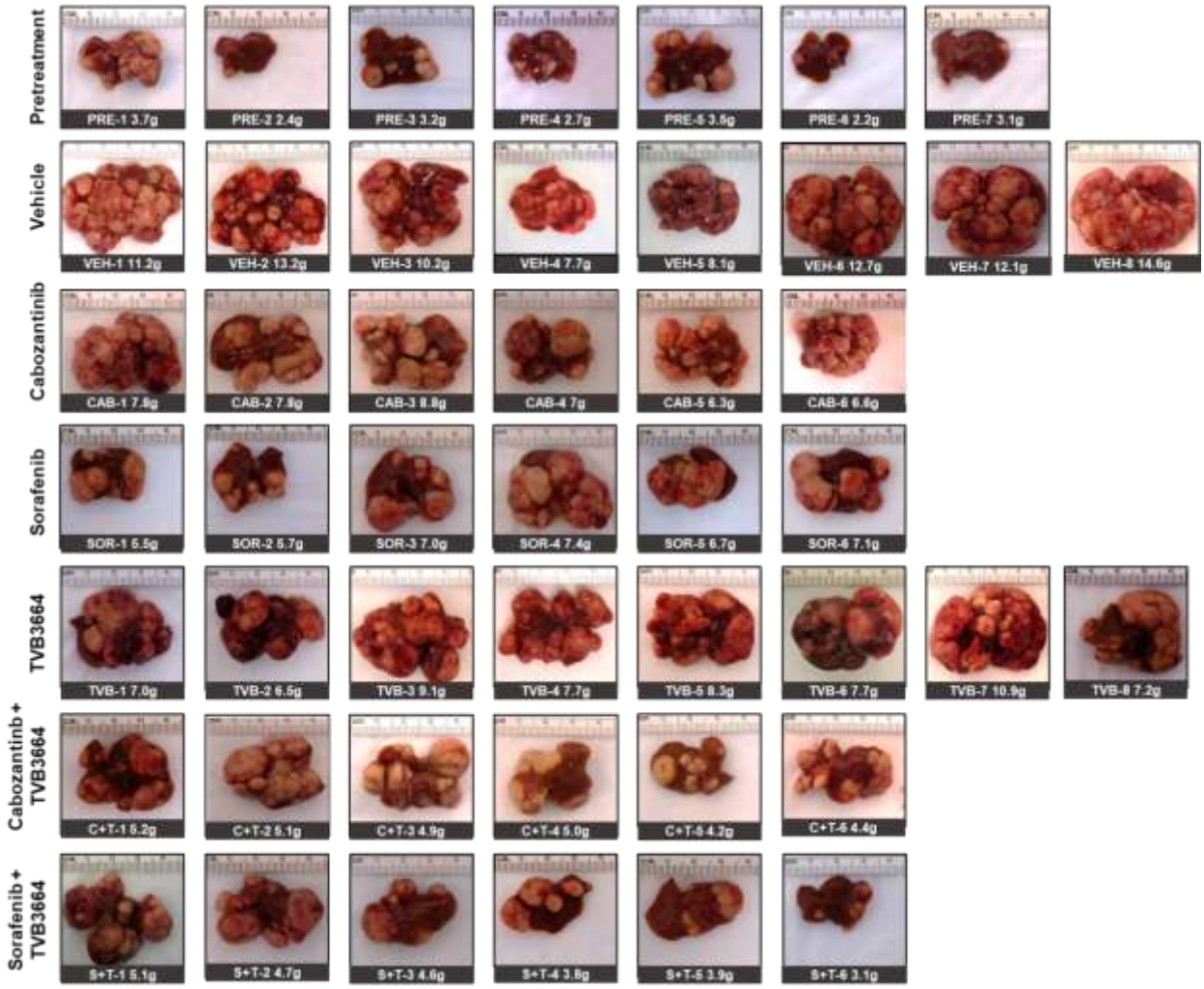

Fig. S23. Macroscopic view of the pretreatment, vehicle-, TVB3664, cabozantinib, sorafenib, cabozantinib/TVB3664, and sorafenib/TVB3664 treated c-MYC tumors. Liver weight is shown at the bottom of each picture. Abbreviations: PRE, pretreatment; VEH, Vehicle; TVB, TVB3664; CAB, cabozantinib; SOR, sorafenib; C+T, cabozantinib/TVB3664, S+T, sorafenib/TVB3664.

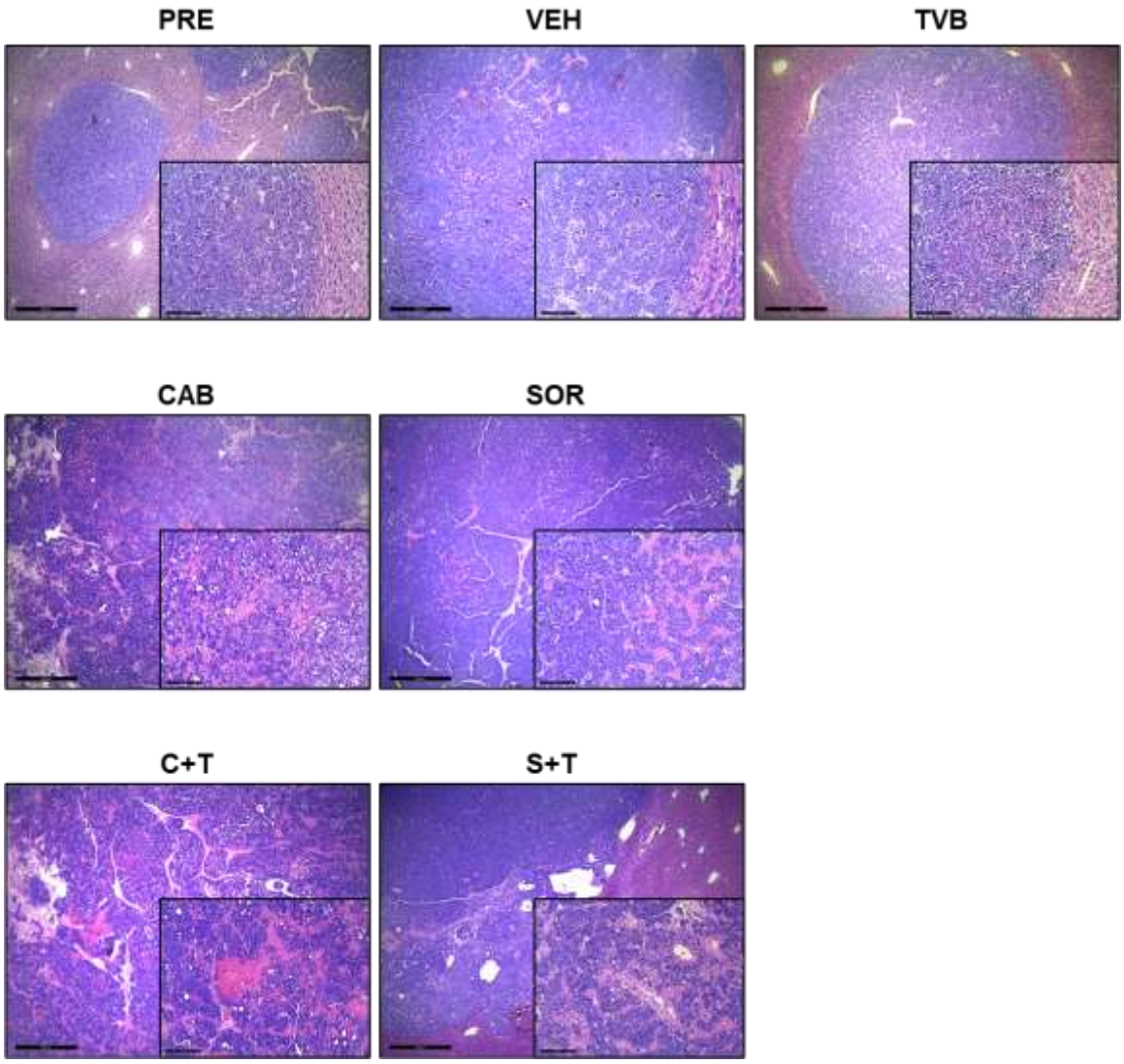

Fig. S24. Representative images of H&E staining in the pretreatment (PRE), vehicle- (VEH), TVB3664 (TVB), cabozantinib (CAB), sorafenib (SOR), cabozantinib/TVB3664 (C+ T), and sorafenib/TVB3664 (S+ T) treated c-MYC tumors. Scale bars: 500µm for 40X (main images) and 100 µm for 200X (insets).

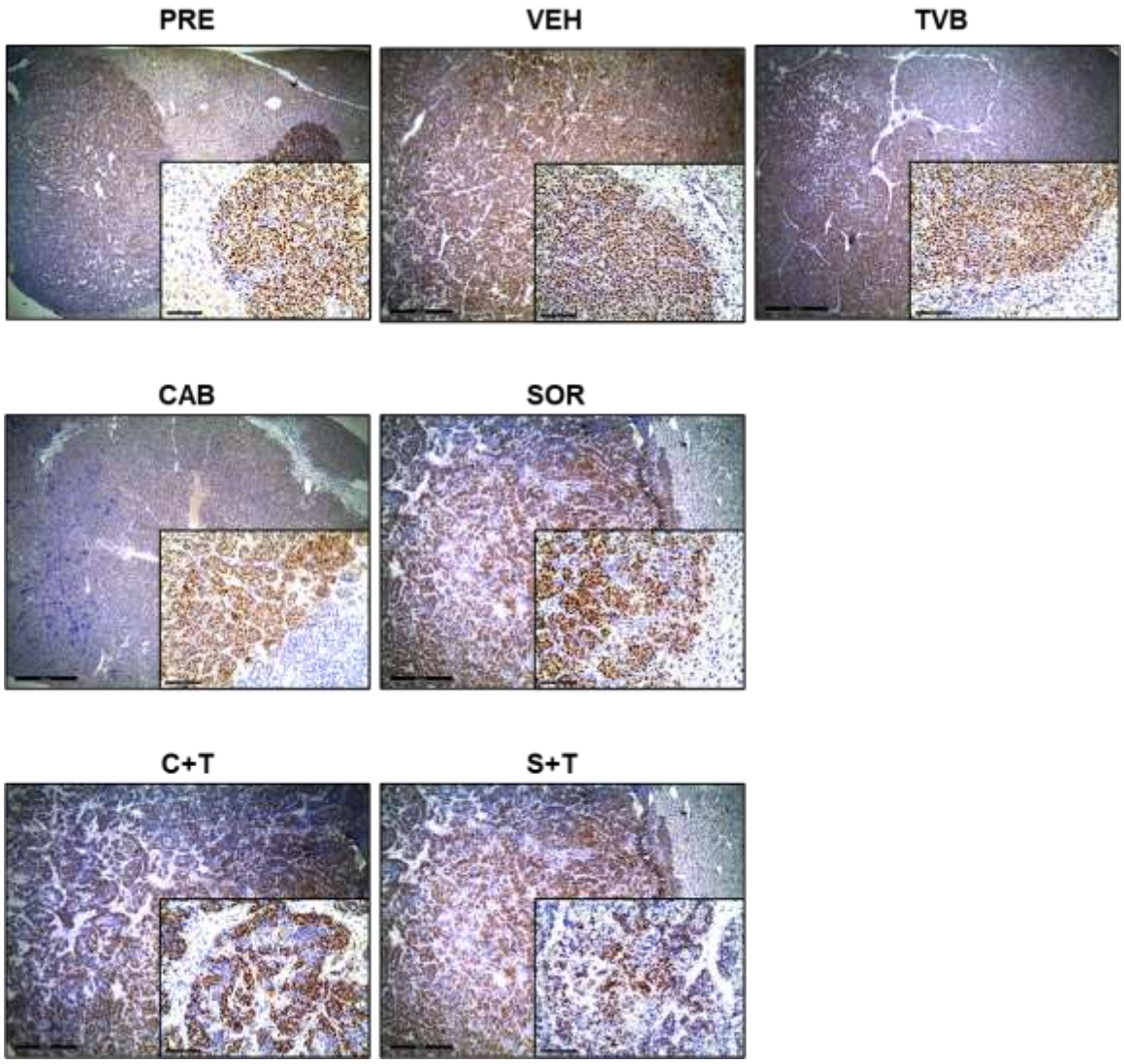

Fig. S25. Representative images of c-MYC staining in the pre-treatment (PRE), vehicle-(VEH), TVB3664 (TVB), cabozantinib (CAB), sorafenib (SOR), cabozantinib/TVB3664 (C+ T), and sorafenib/TVB3664 (S+ T) treated c-MYC tumors. Scale bars: 500µm for 40X (main images) and 100 µm for 200X (insets).

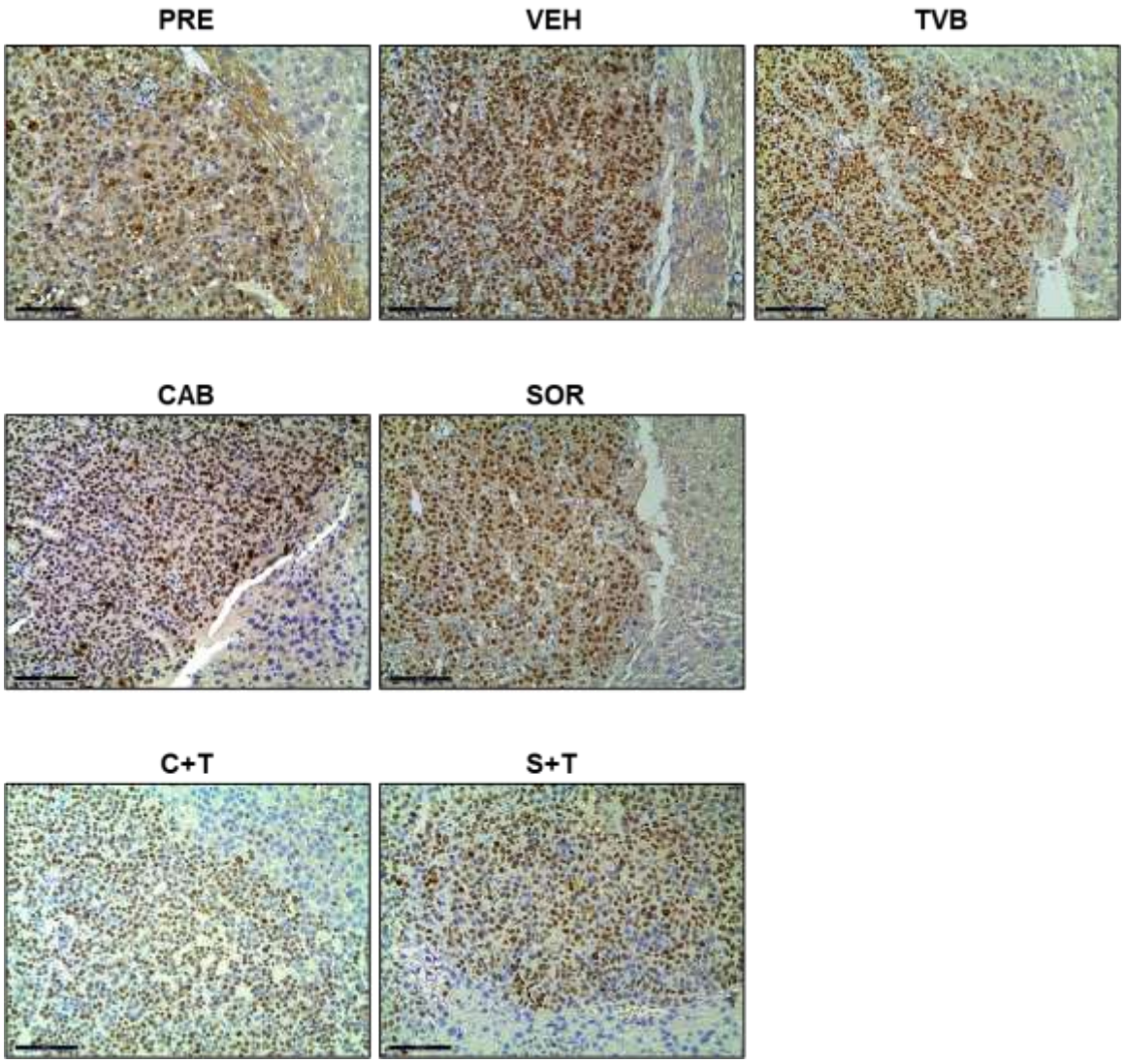

Fig. S26. Representative images of Ki67 staining in the pretreatment (PRE), vehicle- (VEH), TVB3664 (TVB), cabozantinib (CAB), sorafenib (SOR), cabozantinib/TVB3664 (C+ T), and sorafenib/TVB3664 (S+ T) treated c-MYC tumors. Scale bars: 100 μm.

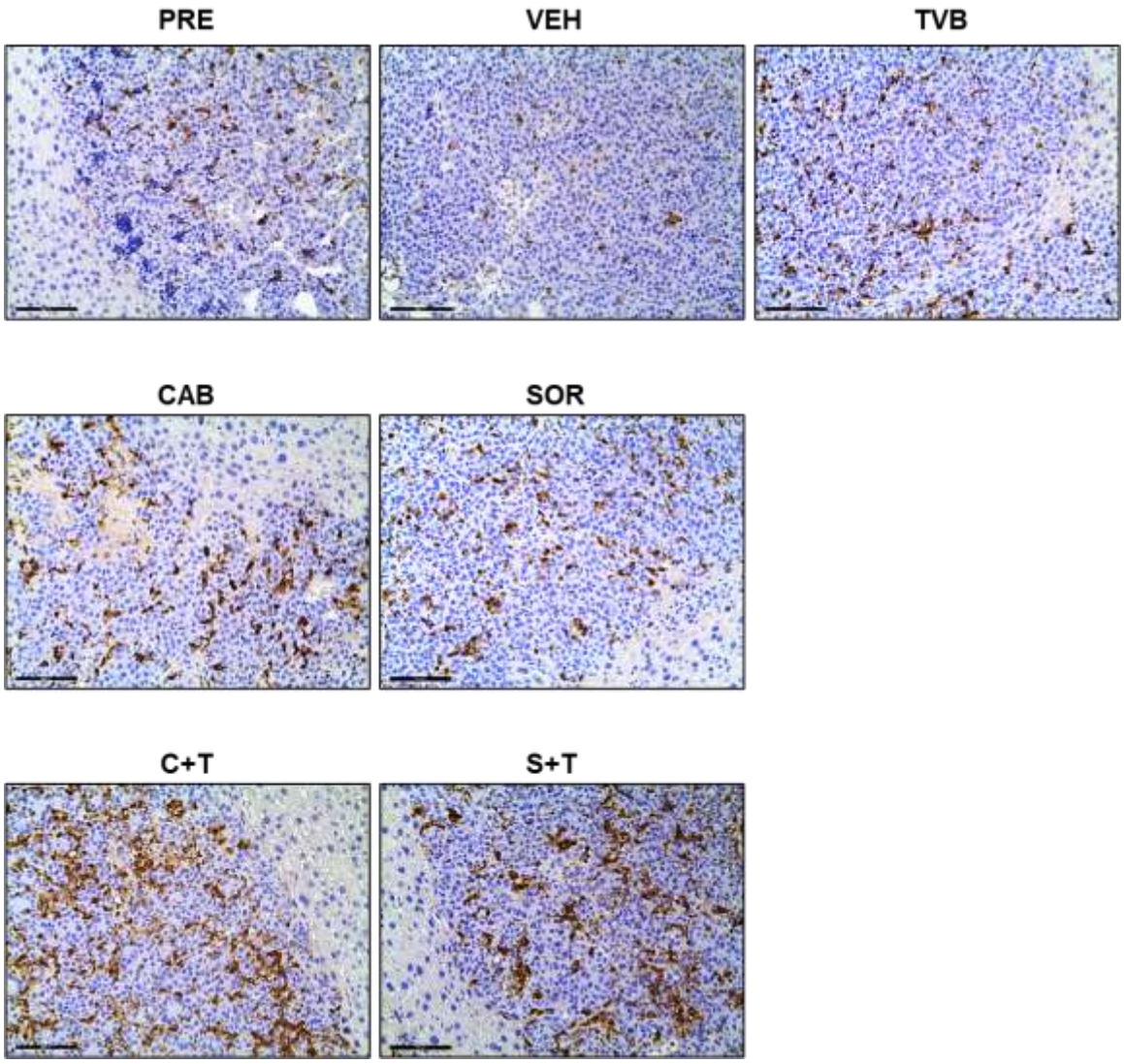

Fig. S27. Representative images of cleaved caspase-3 staining in the pretreatment (PRE), vehicle- (VEH), TVB3664 (TVB), cabozantinib (CAB), sorafenib (SOR), cabozantinib/TVB3664 (C+ T), and sorafenib/TVB3664 (S+ T) treated c-MYC tumors. Scale bars: 100 µm.

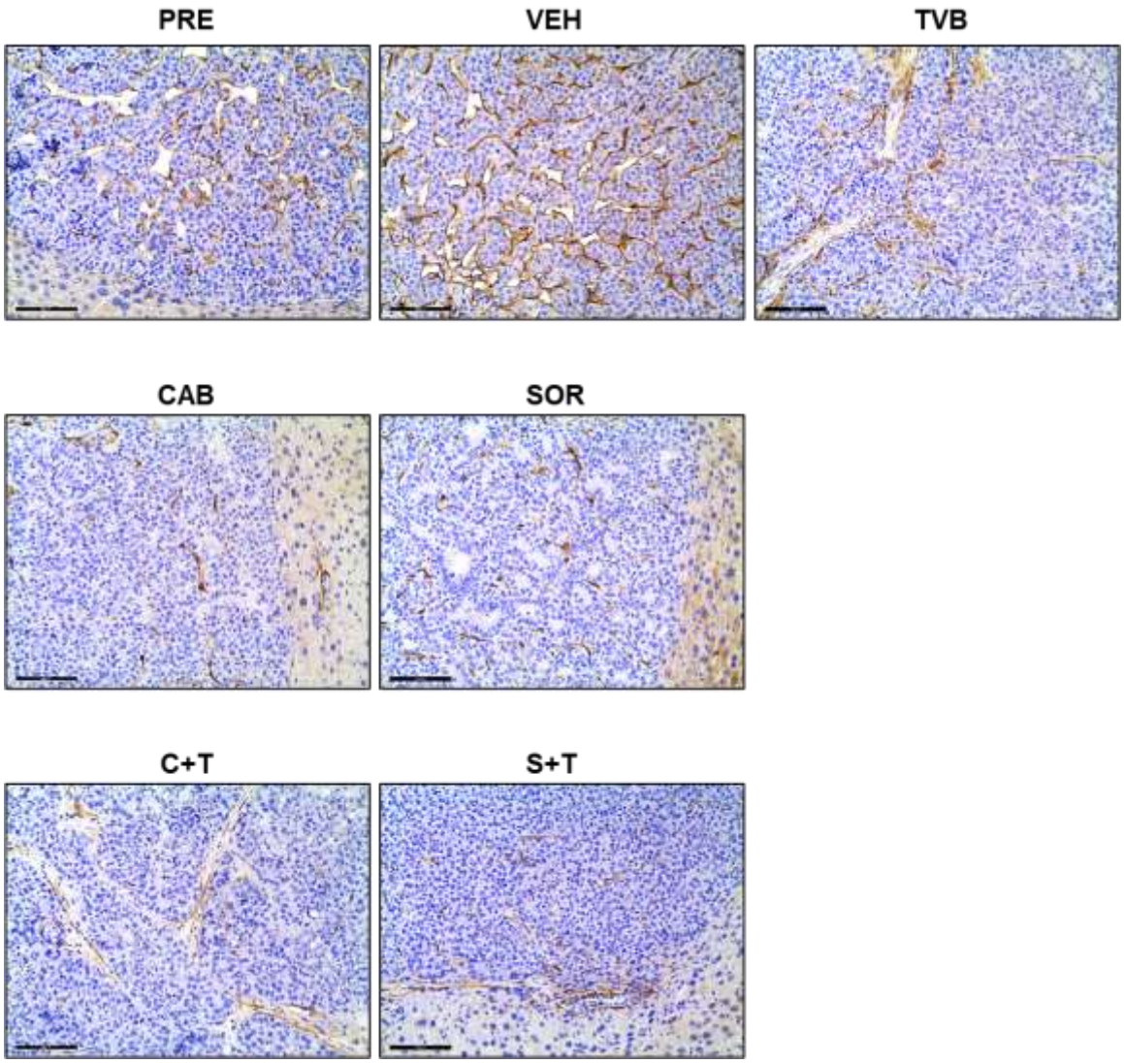

Fig. S28. Representative images of CD34 staining in the pretreatment (PRE), vehicle- (VEH), TVB3664 (TVB), cabozantinib (CAB), sorafenib (SOR), cabozantinib/TVB3664 (C+ T), and sorafenib/TVB3664 (S+ T) treated c-MYC tumors. Scale bars: 100 μm.

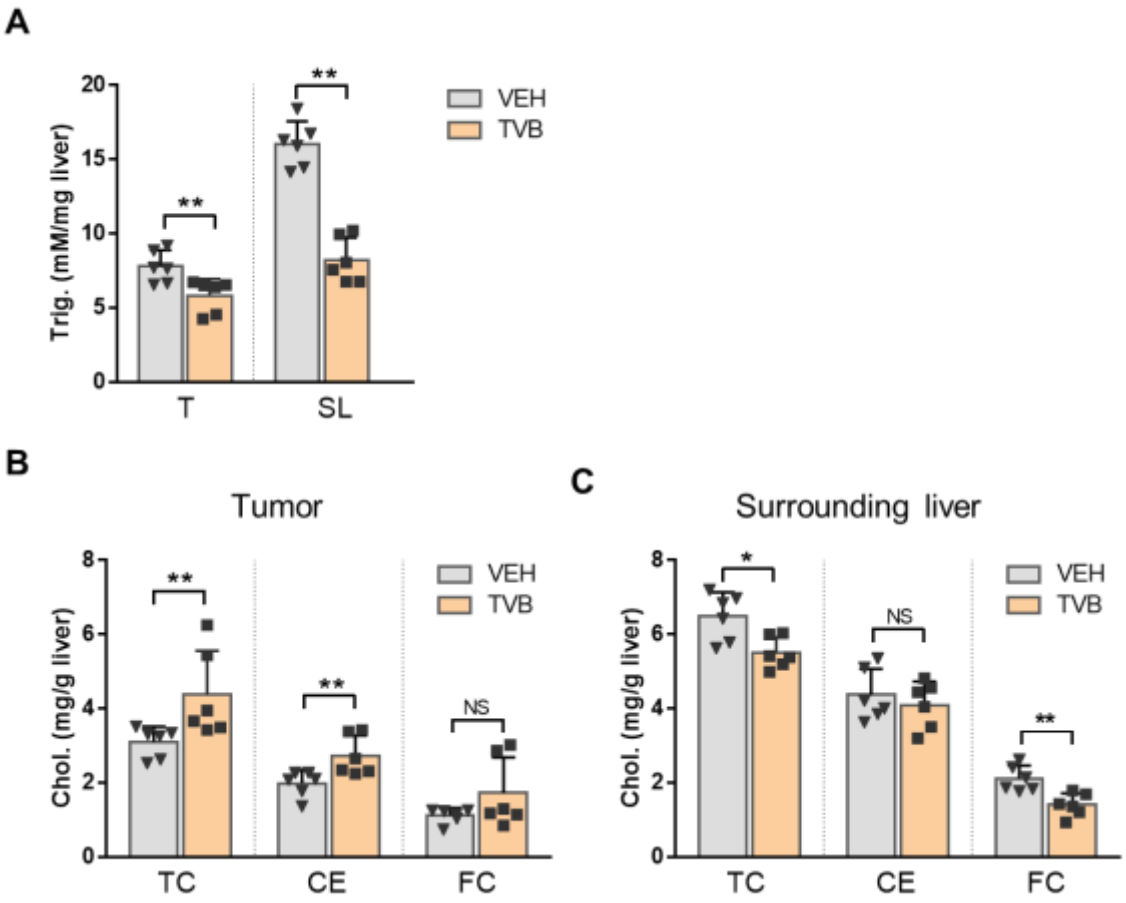

Fig. S29. Analysis of hepatic triglyceride and cholesterol levels in the TVB3664 treated c-MYC mouse HCCs. (A) Hepatic triglyceride levels in the c-MYC tumors (T) and surrounding liver tissues (SL). **(B, C)** Hepatic cholesterol (TC), cholesteryl ester (CE), and free cholesterol (FC) levels in the c-MYC tumors (B) and surrounding tissues (C). * $P < 0.05$; ** $P < 0.01$; NS, no significance. Abbreviations: VEH, Vehicle; TVB, TVB3664.

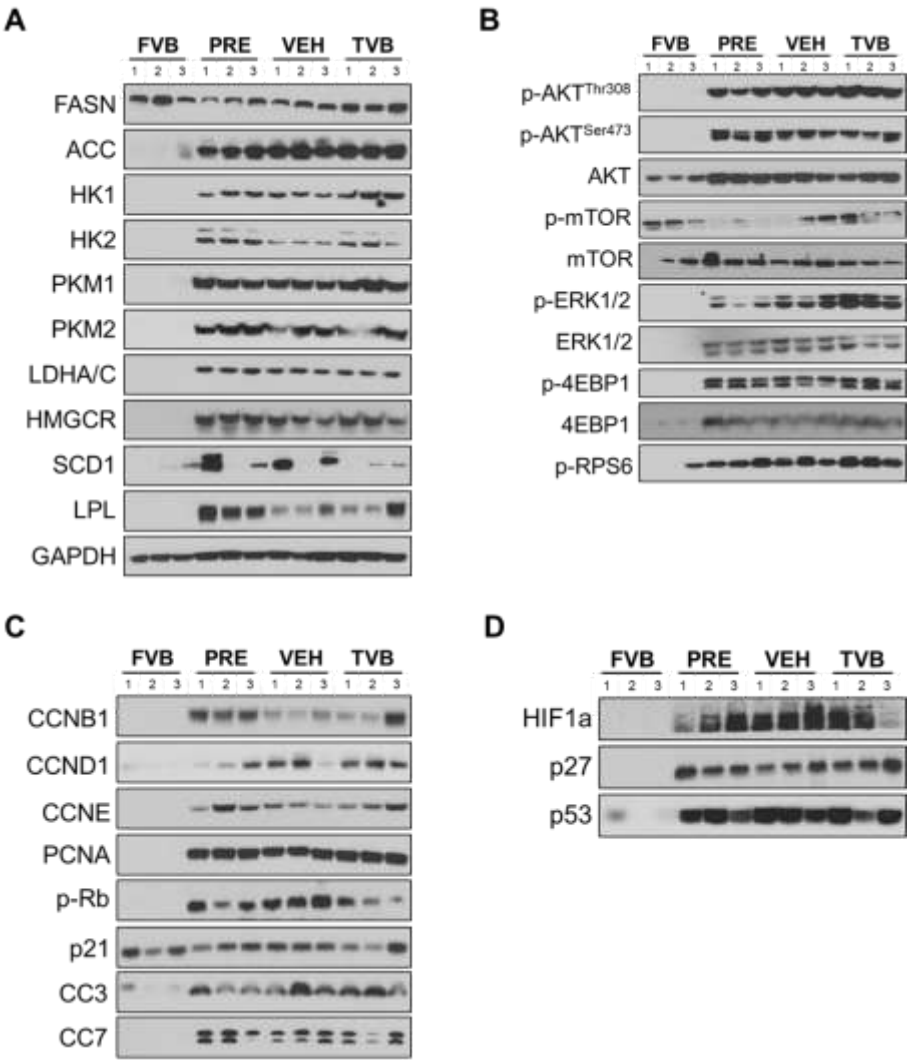

Fig. S30. Effects of TVB3664 on the c-MYC mouse HCC lesions. (A-D) Analysis of fatty acid metabolism-related proteins (A), PI3K/AKT signaling pathway (B), cell cycle and apoptosis-related proteins (C), and other potential TVB3664 targets (D). GAPDH was used as the loading control. Abbreviations: FVB, *FVB/N* wild-type normal liver; PRE, pretreated c-MYC tumors; VEH, Vehicle-treated c-MYC tumors; TVB, TVB3664-treated c-MYC tumors.

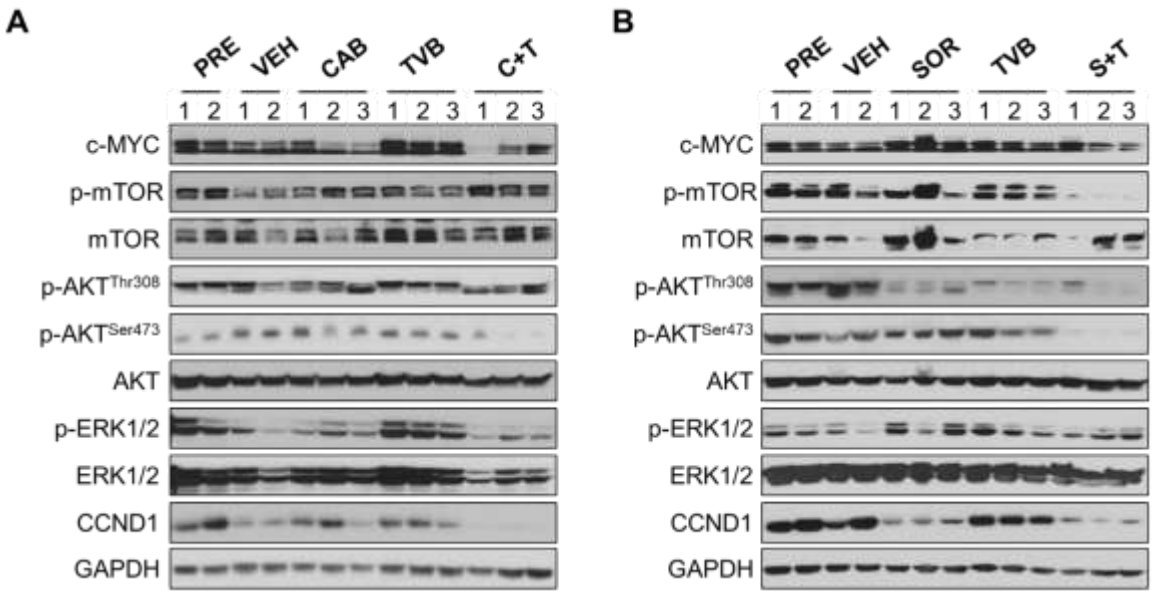

Fig. S31. Effects of TVB3664 and tyrosine kinase inhibitors treatment on the c-MYC mouse HCC lesions. (A) Analysis of PI3K/AKT signaling pathway and cell cycle-related proteins in TVB3664/cabozantinib treated c-MYC tumors. (B) Analysis of PI3K/AKT signaling pathway and cell cycle-related proteins in TVB3664/sorafenib treated c-MYC tumors. GAPDH was used as the loading control. Abbreviations: PRE, pretreatment; VEH, vehicle; TVB, TVB3664; CAB, cabozantinib; SOR, sorafenib; C+T, cabozantinib/TVB3664; S+T, sorafenib/TVB3664.

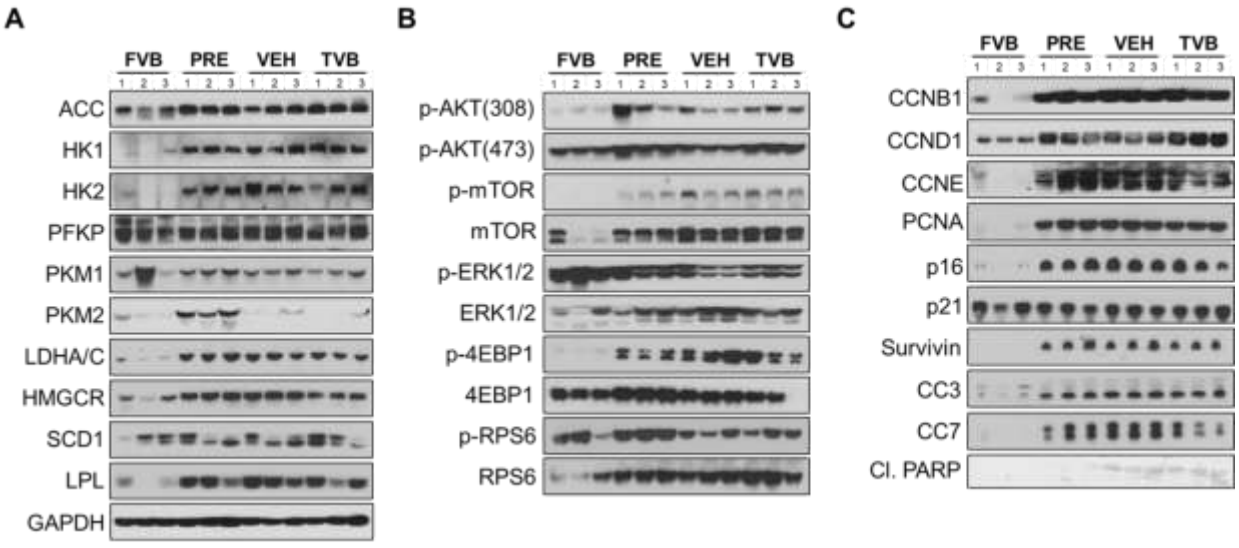

Fig. S32. Effects of TVB3664 on the β-CateninΔ90/c-MET mouse HCC lesions. (A-D) Analysis of fatty acid metabolism-related proteins (A), PI3K/AKT signaling pathway (B), cell cycle, and apoptosis-related (C) proteins. Abbreviations: FVB, *FVB/N* wild-type normal liver; PRE, pretreated β-CateninΔ90/c-MET tumors; VEH, Vehicle-treated β-CateninΔ90/c-MET tumors; TVB, TVB3664-treated β-CateninΔ90/c-MET tumors.

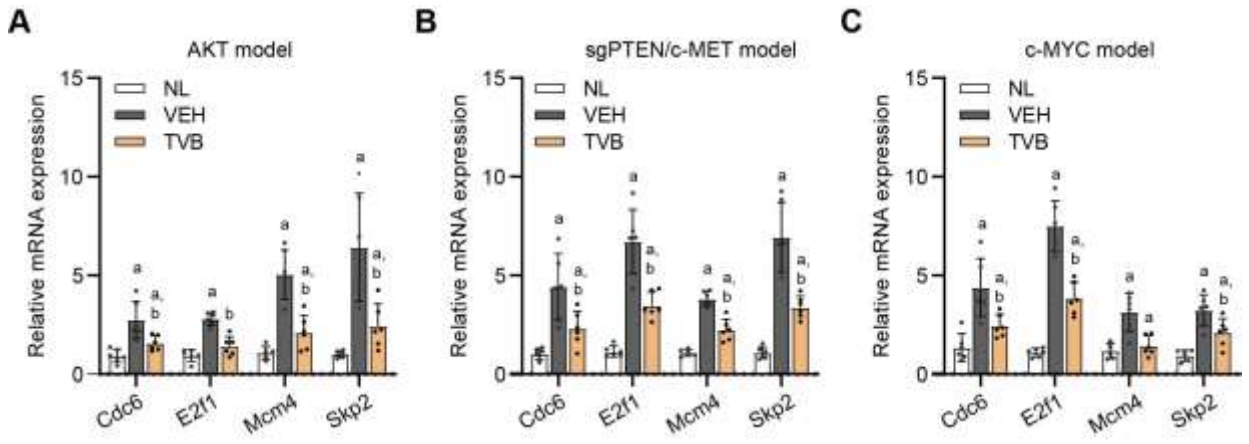

Fig. S33. Analysis of TVB3664 effect on the RB/E2F1 pathway. (A-C) mRNA expressions of *Cdc6, E2f1, Mcm4,* and *Skp2* in the AKT model (A), sgPTEN/c-MET model (B), and c-MYC model (C). $P < 0.05$ (a) vs. NL; (b) vs. VEH. Abbreviations: NL, normal liver; VEH, Vehicle; TVB, TVB3664.

A

Cell line	C75 IC50 (uM)	Cabozantinib IC50 (uM)
MHCC97H	46.93	7.19
HLE	22.55	15.24
SNU449	63.23	35.30

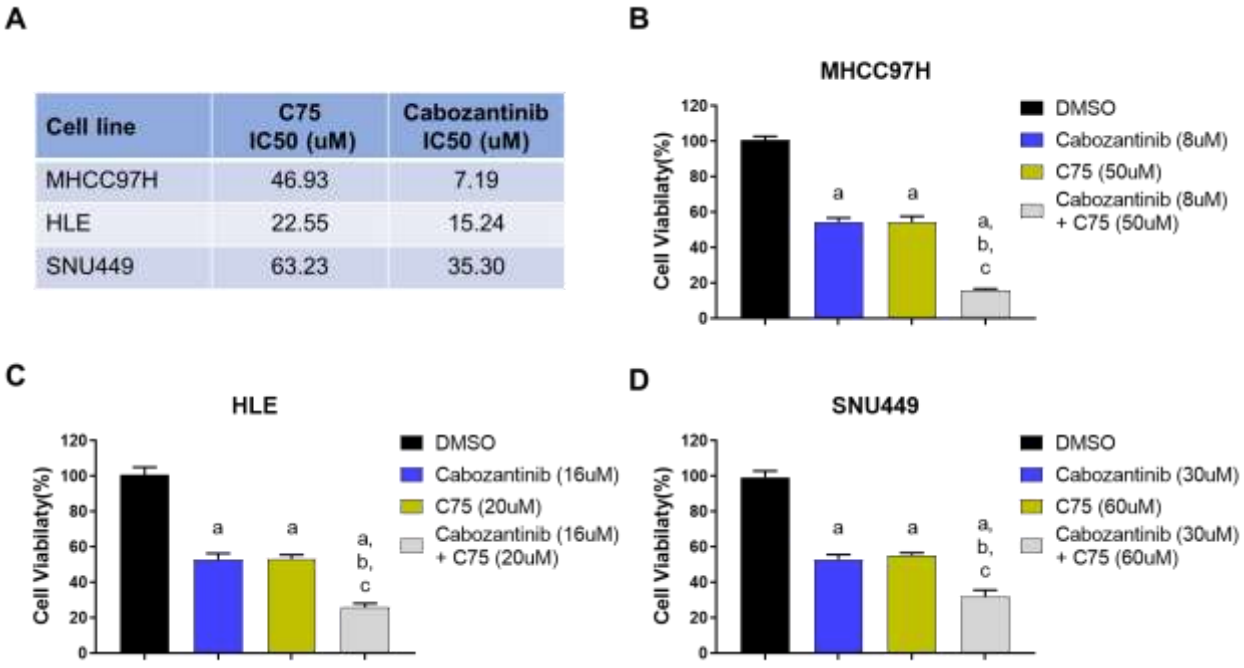

Fig. S34. C75 and cabozantinib concomitant treatment induces growth inhibition in human HCC cell lines. (A) IC50 values of C75 and cabozantinib (same as in Fig. 3) in the MHCC97H, HLE, and SNU449 human HCC cell lines. **(B-D)** Cell viability in the DMSO, cabozantinib, C75, and combinational treated groups with ~IC50 concentrations as indicated in MHCC97H (B), HLE (C), and SNU449 (D) human HCC cells. $P < 0.05$ (a) vs. DMSO; (b) vs. Cabozantinib; (C) vs. C75.

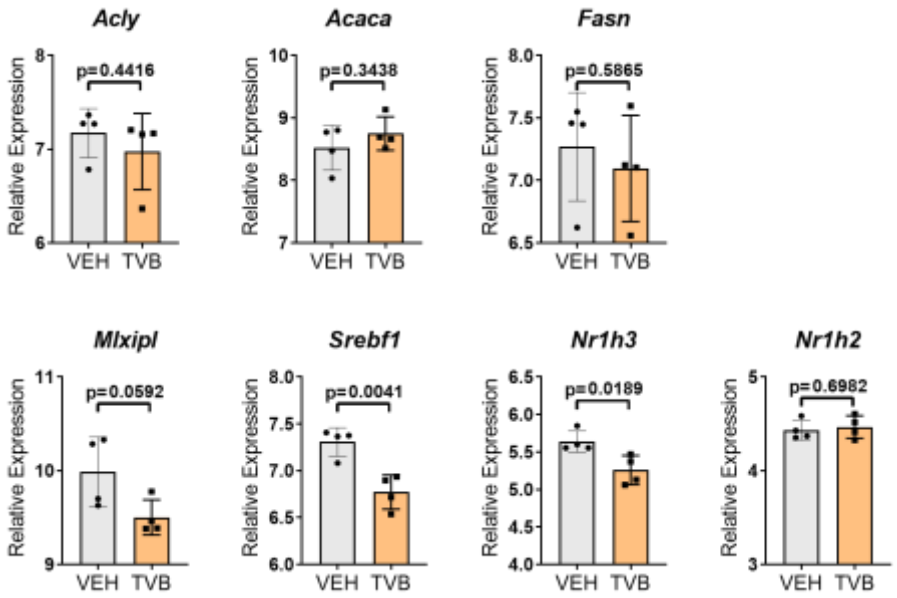

Fig. S35. TVB3664 has minor effects on the expression of *de novo* lipogenesis-related genes. The relative expression (in FPKM) of acetyl-CoA by ATP-citrate lyase (*Acly*), acetyl-CoA carboxylases 1 (ACC1, encoded by *Acaca*), fatty acid synthase (*Fasn*), sterol regulatory element-binding protein 1c (SREBP1c, encoded by *Srebf1*), carbohydrate-response element-binding protein (ChREBP, encoded by *Mlxipl*), liver X receptor alpha (encoded by *Nr1h3*), and liver X receptors beta (encoded by *Nr1h2*) in the sgPTEN/c-MET tumors treated with vehicle and TVB3664. Abbreviations: VEH, Vehicle; TVB, TVB3664.

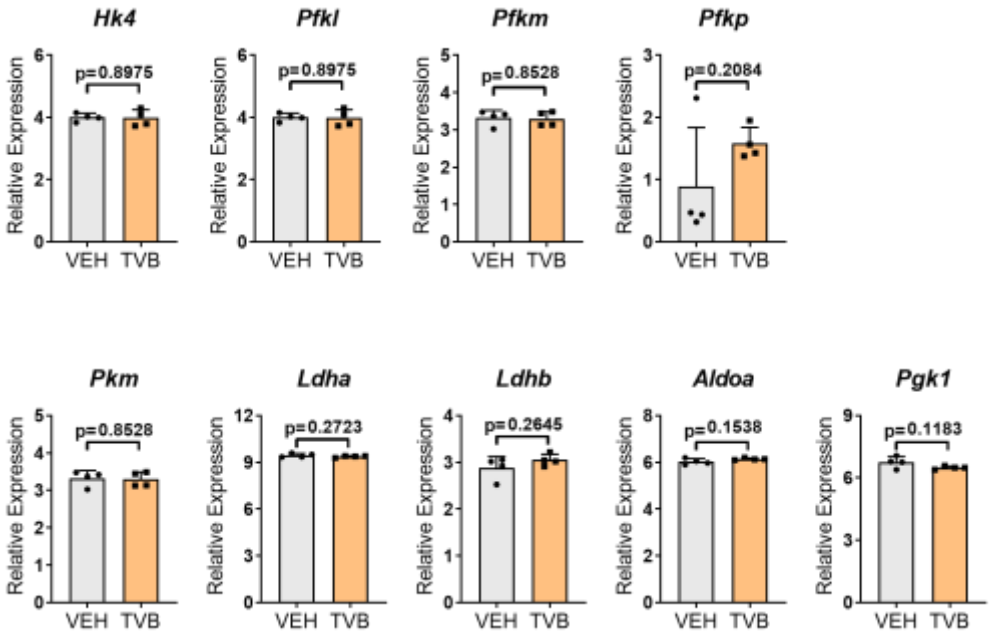

Fig. S36. TVB3664 does not affect the expression of genes encoding glycolytic enzymes. The relative expression (in FPKM) of *Hk4, Pfkl, Pfkm, Pfkp, Pkm, Ldha, Ldhb, Aldoa, Pgk1* in the sgPTEN/c-MET tumors treated with vehicle and TVB3664. Abbreviations: VEH, Vehicle; TVB, TVB3664.

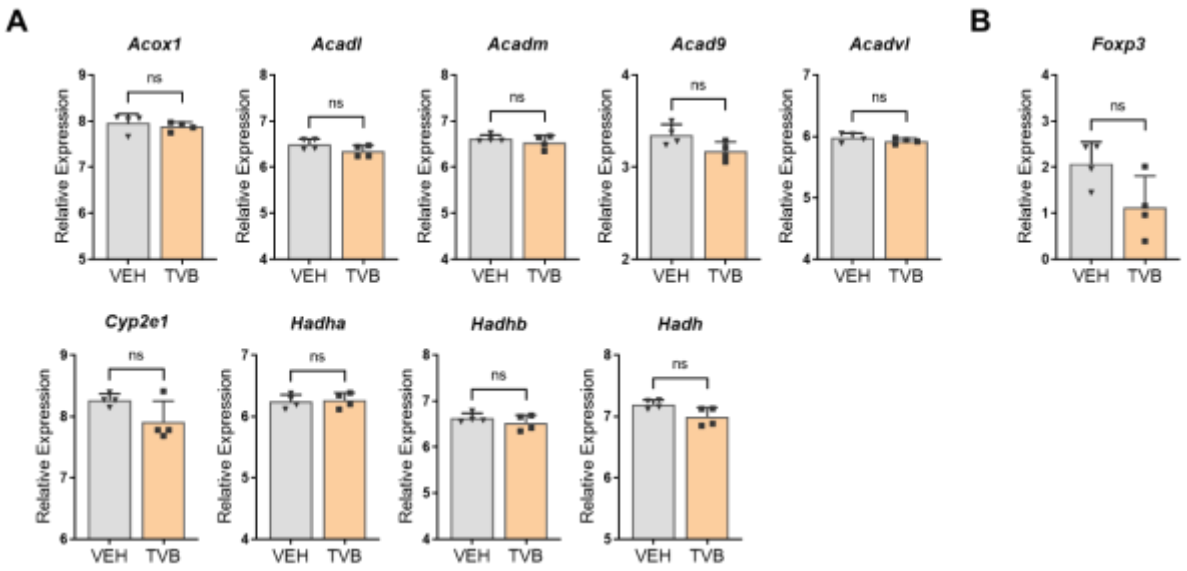

Fig. S37. TVB3664 does not affect the expression of genes in the fatty acid β-oxidation cycle or Foxp3. **(A)** The relative expression (in FPKM) of very long-chain acyl-CoA dehydrogenase (*Acadvl*), long-chain acyl-CoA dehydrogenase (*Acadl*), medium-chain acyl-CoA dehydrogenase (*Acadm*), acyl-CoA dehydrogenase 9 (*Acad9*), acyl-CoA oxidase 1 (*Acox1*), cytochrome P450 family 2 subfamily E member 1(*Cyp2e1*), mitochondrial trifunctional protein, alpha subunit (*Hadha*), mitochondrial trifunctional protein, beta subunit (*Hadhb*) and hydroxyacyl-coenzyme A dehydrogenase (*Hadh*) in the sgPTEN/c-MET tumors treated with vehicle and TVB3664. **(B)** The relative expression (in FPKM+3) of *Foxp3* in the sgPTEN/c-MET tumors treated with vehicle and TVB3664. Abbreviations: VEH, Vehicle; TVB, TVB3664; NS, no significance.

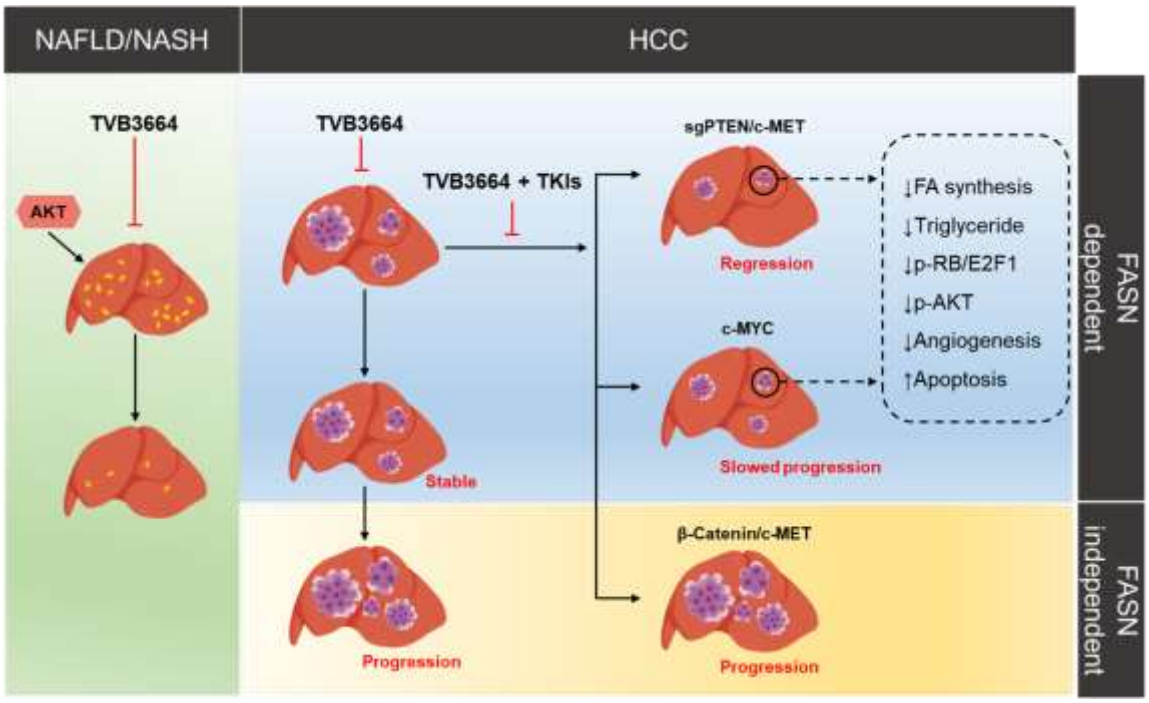

Fig. S38. Graphical abstract. TVB3664 effectively inhibits *de novo* lipogenesis and improves NAFLD/NASH-related effects in old mice and AKT overexpressing livers. TVB3664 monotherapy showed moderate efficacy in NASH-related murine HCCs, induced by loss of PTEN and c-MET overexpression. TVB3664, in combination with cabozantinib, triggered tumor regression in this mouse HCC model. TVB3664 also improved the therapeutic efficacy of sorafenib and cabozantinib in the FASN-dependent c-MYC HCC model. However, TVB3664 had no efficacy nor synergistic effects in FASN-independent mouse HCC models.